

Li abundances in F stars: planets, rotation, and Galactic evolution^{★,★★}

E. Delgado Mena^{1,2}, S. Bertrán de Lis^{3,4}, V. Zh. Adibekyan^{1,2}, S. G. Sousa^{1,2}, P. Figueira^{1,2}, A. Mortier⁶, J. I. González Hernández^{3,4}, M. Tsantaki^{1,2,3}, G. Israelian^{3,4}, and N. C. Santos^{1,2,5}

¹ Centro de Astrofísica, Universidade do Porto, Rua das Estrelas, 4150-762 Porto, Portugal
e-mail: Elisa.Delgado@astro.up.pt

² Instituto de Astrofísica e Ciências do Espaço, Universidade do Porto, CAUP, Rua das Estrelas, 4150-762 Porto, Portugal

³ Instituto de Astrofísica de Canarias, C/via Lactea, s/n, 38200 La Laguna, Tenerife, Spain

⁴ Departamento de Astrofísica, Universidad de La Laguna, 38205 La Laguna, Tenerife, Spain

⁵ Departamento de Física e Astronomia, Faculdade de Ciências, Universidade do Porto, Portugal

⁶ SUPA, School of Physics and Astronomy, University of St. Andrews, St. Andrews KY16 9SS, UK

Received 28 November 2014 / Accepted 14 December 2014

ABSTRACT

Aims. We aim, on the one hand, to study the possible differences of Li abundances between planet hosts and stars without detected planets at effective temperatures hotter than the Sun, and on the other hand, to explore the Li dip and the evolution of Li at high metallicities.

Methods. We present lithium abundances for 353 main sequence stars with and without planets in the T_{eff} range 5900–7200 K. We observed 265 stars of our sample with HARPS spectrograph during different planets search programs. We observed the remaining targets with a variety of high-resolution spectrographs. The abundances are derived by a standard local thermodynamic equilibrium analysis using spectral synthesis with the code MOOG and a grid of Kurucz ATLAS9 atmospheres.

Results. We find that hot jupiter host stars within the T_{eff} range 5900–6300 K show lower Li abundances, by 0.14 dex, than stars without detected planets. This offset has a significance at the level 7σ , pointing to a stronger effect of planet formation on Li abundances when the planets are more massive and migrate close to the star. However, we also find that the average $v \sin i$ of (a fraction of) stars with hot jupiters is higher on average than for single stars in the same T_{eff} region, suggesting that rotational-induced mixing (and not the presence of planets) might be the cause for a greater depletion of Li. We confirm that the mass-metallicity dependence of the Li dip is extended towards $[\text{Fe}/\text{H}] \sim 0.4$ dex (beginning at $[\text{Fe}/\text{H}] \sim -0.4$ dex for our stars) and that probably reflects the mass-metallicity correlation of stars of the same T_{eff} on the main sequence. We find that for the youngest stars (< 1.5 Gyr) around the Li dip, the depletion of Li increases with $v \sin i$ values, as proposed by rotationally-induced depletion models. This suggests that the Li dip consists of fast rotators at young ages whereas the most Li-depleted old stars show lower rotation rates (probably caused by the spin-down during their long lives). We have also explored the Li evolution with $[\text{Fe}/\text{H}]$ taking advantage of the metal-rich stars included in our sample. We find that Li abundance reaches its maximum around solar metallicity, but decreases in the most metal-rich stars, as predicted by some models of Li Galactic production.

Key words. stars: abundances – stars: fundamental parameters – stars: rotation – stars: evolution – planets and satellites: formation – planetary systems

1. Introduction

Lithium is one of the most studied chemical elements in the literature. Despite efforts to unveil the mechanisms of production and destruction of this interesting element, there are still some unsolved mysteries. For instance, the disagreement found between

the abundance of the most metal-poor stars in the Galaxy (the so-called “Spite plateau” with $A(\text{Li})^1 \sim 2.2$, Spite & Spite 1982) and the initial primordial abundance given by the WMAP observations ($A(\text{Li}) \sim 2.7$, Steigman 2010, Cyburt et al. 2008) is not understood yet. Moreover, the current Galactic Li production models (e.g. Prantzos 2012) are not able to yield enough Li to explain the meteoritic abundance of 3.31 (Anders & Grevesse 1989) or the maximum Li abundances found in young clusters (e.g. Sestito & Randich 2005). On the other hand, the standard model of Li depletion, which only considers convection (e.g. Deliyannis et al. 1990; Pinsonneault 1997) cannot explain the observed Li abundances in solar-type stars or in mid-F stars that have undergone the Li dip. Furthermore, in previous years a new discussion about the effect of planets on the depletion of Li has

* Based on observations collected at the La Silla Observatory, ESO (Chile), with the HARPS spectrograph at the 3.6 m ESO telescope, with CORALIE spectrograph at the 1.2 m Euler Swiss telescope and with the FEROS spectrograph at the 1.52 m ESO telescope; at the Paranal Observatory, ESO (Chile), using the UVES spectrograph at the VLT/UT2 Kueyen telescope, and with the FIES and SARG spectrographs at the 2.5 m NOT and the 3.6 m TNG, respectively, both at La Palma (Canary Islands, Spain).

** Tables 3–6 are available in electronic form at
<http://www.aanda.org>

¹ $A(\text{Li}) = \log[N(\text{Li})/N(\text{H})] + 12$.

Table 1. Parameters for each coefficient as resulting from multivariable linear regression analysis in the four tests (PH are planet hosts and CS are the comparison stars).

Sample of planet hosts	Number	Int.	β_1	β_2	β_3	β_4	β_5	Offset	Significance
Jupiter size hosts	87PH & 176CS	-64.04	17.81	0.02	-0.18	-0.21		-0.07	6.5σ
Hot jupiter hosts	24PH & 176CS	-69.64	19.37	-0.05	-0.24	-0.28		-0.14	7.0σ
Analysis including $v \sin i$									
Jupiter size hosts	47PH & 62CS	-86.39	23.72	0.06	-0.10	-0.20	-0.12	0.04	2.6σ
Hot jupiter hosts	11PH & 62CS	-98.37	27.16	-0.05	-0.29	-0.28	-0.15	0.08	2.1σ

Notes. The offset is only included in the fit for planet hosts since the offset for comparison stars is by definition 0. The last column reflects the significance of the offset found between both samples.

been opened (e.g. Israeli et al. 2009; Ramírez et al. 2012; Gonzalez 2014; Figueira et al. 2014; Delgado Mena et al. 2014, hereafter DM14).

Lithium, as other light elements, can easily be destroyed in stellar interiors by p- α reactions. Although Li depletion occurs primarily in the pre-main sequence (PMS), it can also take place in stellar envelopes if there is any extra mixing process. Therefore, Li abundance can provide us important information about the internal structure of stars. In this work we present homogeneous Li abundances for a sample of 353 “hot” stars (early G and F stars) with a wide range of metallicities and ages. We exploit the metal-rich stars in our sample to study the behaviour of the Li dip and the chemical evolution of Li at high metallicities. Finally, we also investigate if the presence of planets affect Li abundances for these hotter stars.

Section 2 briefly describes the collected data together with the determination of stellar parameters and abundances of lithium. In Sect. 3 we discuss the results related to different topics: the connection of Li abundances with the presence of planets, the behaviour of the Li dip, the chemical evolution of Li at high metallicities, and the Li distribution in the Galactic disks. We summarize in Sect. 4.

2. Observations and analysis

Our baseline sample is 1111 FGK stars observed within the context of the HARPS GTO programs. It is a combination of three HARPS subsamples hereafter called HARPS-1 (Mayor et al. 2003), HARPS-2 (Lo Curto et al. 2010), and HARPS-4 (Santos et al. 2011). The individual spectra of each star were reduced using the HARPS pipeline and then combined with IRAF² after correcting for its radial velocity shift. The final spectra have a resolution of $R \sim 110\,000$ and high signal-to-noise ratio (55% of the spectra have a S/N higher than 200). The total sample is composed of 135 stars with planets and 976 stars without detected planets. For this work, we mainly focus on the hottest T_{eff} (>5900 K) where we have 36 and 229 stars with and without planets, respectively. All the planet hosts and non-hosts stars are listed in Tables 3 and 4, respectively. To increase the number of stars with planets, we used high-resolution spectra for 88 planet hosts (see Table 5) that come from different observing runs and spectrographs. Table 1 of DM14 lists those instruments in detail. The data reduction was made using the IRAF package or the respective telescopes pipelines. All the images were flat-field corrected, sky subtracted, and co-added to obtain 1D spectra. Doppler correction was also done.

² IRAF is distributed by National Optical Astronomy Observatories, operated by the Association of Universities for Research in Astronomy, Inc., under contract with the National Science Foundation, USA.

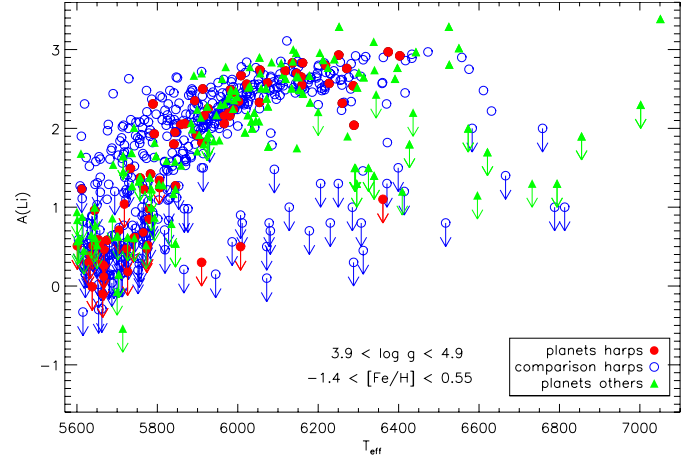


Fig. 1. Lithium abundances vs. T_{eff} for planet host stars (red filled circles) and comparison sample stars (blue open circles) from HARPS together with other planet hosts (green triangles). Down arrows represent $A(\text{Li})$ upper limits.

The stellar atmospheric parameters were taken from Sousa et al. (2008, 2011a,b) for the HARPS samples and from Santos et al. (2004, 2005), Sousa et al. (2006), Mortier et al. (2013), Santos et al. (2013) for the rest of the planet hosts. All the sets of parameters were determined in a homogeneous way. We derived lithium abundances $A(\text{Li})$, stellar masses and ages in the same way as DM14. That work offers further details about the determination of stellar parameters and Li abundances.

The determination of rotational projected velocities ($v \sin i$ values) was done with a combined Fourier transform and goodness-of-fit methodology using the IACOB program (Simón-Díaz & Herrero 2014). We could only determine $v \sin i$ for the stars with spectra of S/Ns above ~ 100 .

3. Results and discussion

3.1. General behaviour of Li in F stars

In Fig. 1 we present a general overview of the Li abundances as a function of effective temperature for our sample. The ranges in [Fe/H] and gravity for the stars in this sample are specified in the plot. To better appreciate the behaviour of Li in a wider T_{eff} range, we have also included the solar-type stars from DM14, with $5600 \text{ K} < T_{\text{eff}} < 5900 \text{ K}$. As expected, Li abundances decrease as the stars get cooler because of their thicker convective envelopes. However, for higher T_{eff} , we still observe an important number of stars with a strong destruction of Li. The stars around 6400 K belong to the well-known Li dip, which was first discovered in the Hyades cluster by Boesgaard & Tripicco (1986), but those with cooler temperatures, between 5900 K

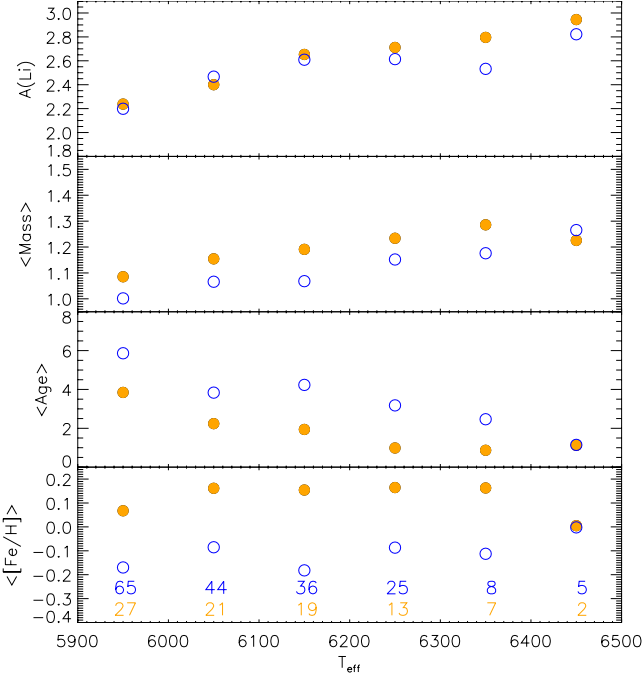


Fig. 2. Average of $A(\text{Li})$, stellar mass, age, and $[\text{Fe}/\text{H}]$ in six T_{eff} bins for all (HARPS+others) the planet host stars (orange filled circles) and comparison sample stars (blue open circles). The number of stars in each bin is indicated with the respective colour. Only stars with Li detections are considered.

and 6200 K, are not so common in studies of clusters or field stars. We would expect these stars to have higher Li abundances unless they are evolved stars from the dip, as suggested by Chen et al. (2001). These objects will be further studied in a separate work. Although we do not expect to have evolved stars in our sample we have removed the stars with $\log g < 4.2$ since our spectroscopic $\log g$ values could be overestimated for the hottest stars (Mortier et al. 2014).

3.2. Li and planets

The Li dependence on the presence of planets has been extensively discussed in the literature. On the one hand, several independent groups find that planet hosts with T_{eff} close to solar present lower abundances of Li when compared to non-hosts (Israelian et al. 2004, 2009; Takeda & Kawanomoto 2005; Chen & Zhao 2006; Gonzalez 2008, 2014; Takeda et al. 2010; Gonzalez et al. 2010; Sousa et al. 2010; Delgado Mena et al. 2014; Figueira et al. 2014). On the other hand, other authors do not find such a dependence (Ryan 2000; Luck & Heiter 2006; Baumann et al. 2010; Ghezzi et al. 2010; Ramírez et al. 2012). Gonzalez (2008) proposed that stars with planets around 6100 K show higher Li abundances than stars without detected planets. After increasing the sample size, however, the same author discarded this effect and presented weak evidence that planet hosts at $T_{\text{eff}} \sim 6100$ –6200 K are deficient in Li compared to stars without detected planets (Gonzalez 2014, 2015). Visually we cannot pinpoint any strong difference in the Li abundance detections between stars with and without planets in Fig. 1. However it is very clear that in the T_{eff} range between 5900 K and 6300 K there are relatively more non-hosts with upper limits in Li abundances. This feature was also pointed out by Ramírez et al. (2012).

In Fig. 2 we compile the average values of Li abundance detections and other parameters for stars with and without detected

planets (in bins of 100 K). Since Li abundances depend on several parameters (e.g. T_{eff} , $[\text{Fe}/\text{H}]$, age) one should be cautious when comparing stars and construct the least biased possible samples (for a further discussion see DM14). For example, in all these subsamples except the hottest one, planet hosts are younger and also on average more metal rich, as expected (e.g. Santos et al. 2004). Nevertheless, this difference in parameters does not seem to affect the degree of Li depletion too much (see Sect. 3.4), except maybe in the T_{eff} range 6300–6400 K where we observe the highest difference in Li. For the rest of the subsamples, the average values of stars with and without planets are quite similar and within the errors.

To remove the effect of different stellar parameters when comparing Li abundances, we apply a multivariate regression fit to the planet host sample and the comparison sample as done in Figueira et al. (2014):

$$\log(A(\text{Li})) = \text{int.} + \beta_1 \log(T_{\text{eff}}) + \beta_2 [\text{Fe}/\text{H}] + \beta_3 \log g + \beta_4 \log(\text{Age}) + M \times \text{offset.} \quad (1)$$

In both samples, we assumed the same linear dependence of Li on stellar parameters but allow an offset for the planet host sample, which is, $M = 0$ for the comparison sample and $M = 1$ for the planet host sample. By doing so, we ensure that a possible difference in Li abundance is not due to different stellar parameters. For this calculation we consider all our stars with $5900 \text{ K} < T_{\text{eff}} < 6300 \text{ K}$ and Li detections (we exclude the upper limits), 87 planet hosts (with Jupiter type planets: $M_p \geq 0.1 M_J$) and 176 comparison stars. We chose to cut at $T_{\text{eff}} = 6300 \text{ K}$ to allow for a fair comparison with the Gonzalez (2015) sample. Moreover, that is roughly the temperature at which the Li dip begins to develop and it would be difficult to distinguish a possible effect of planets on Li abundances from other depletion mechanisms.

The results are shown in Table 1. As expected, the strongest dependence lies on T_{eff} , while it is very small for the other parameters. We find that the planet host sample shows a depletion of 0.07 dex with respect to non-hosts. Although this offset is significant (at 6.5σ level), its significance is naturally heavily dependent on the error bars. If we artificially increase the error bars by a factor of 2 or 3 the significance drops to 3.3σ and 2.2σ , respectively. This offset agrees with the results by Gonzalez (2015) though it is very small and at the level of the uncertainties³. Therefore, it seems that the effect of giant planets observed for solar analogues is not obvious for hotter stars, probably because of their shallower convective envelopes. As explained in DM14, the effect of planets on Li abundances is expected to be higher for more massive planets (stronger effect on rotational history, Bouvier 2008), and for planets that migrate (more violent accretion bursts, Baraffe & Chabrier 2010). Thus, we explore the behaviour of stars hosting hot jupiters since these planets are massive and some theories of planet formation predict a migration close to the star (e.g. Alibert et al. 2005). Then, we repeat our previous calculation, instead using as planet host sample only those stars that host planets with $M > 0.1 M_J$ and $P < 5$ days. In this case we find a higher offset than before, -0.14 dex, with a significance level of 7σ . As before, we increase the error bars by a factor of 2 and 3, which drops the significance to 3.6σ and 2.4σ , respectively. We note that our sample of hot jupiter hosts is small (24 stars with $5900 \text{ K} < T_{\text{eff}} < 6300 \text{ K}$), but this is an interesting result that deserves to be explored further in the future.

³ The average uncertainty in Li abundances for our stars is 0.07 dex.

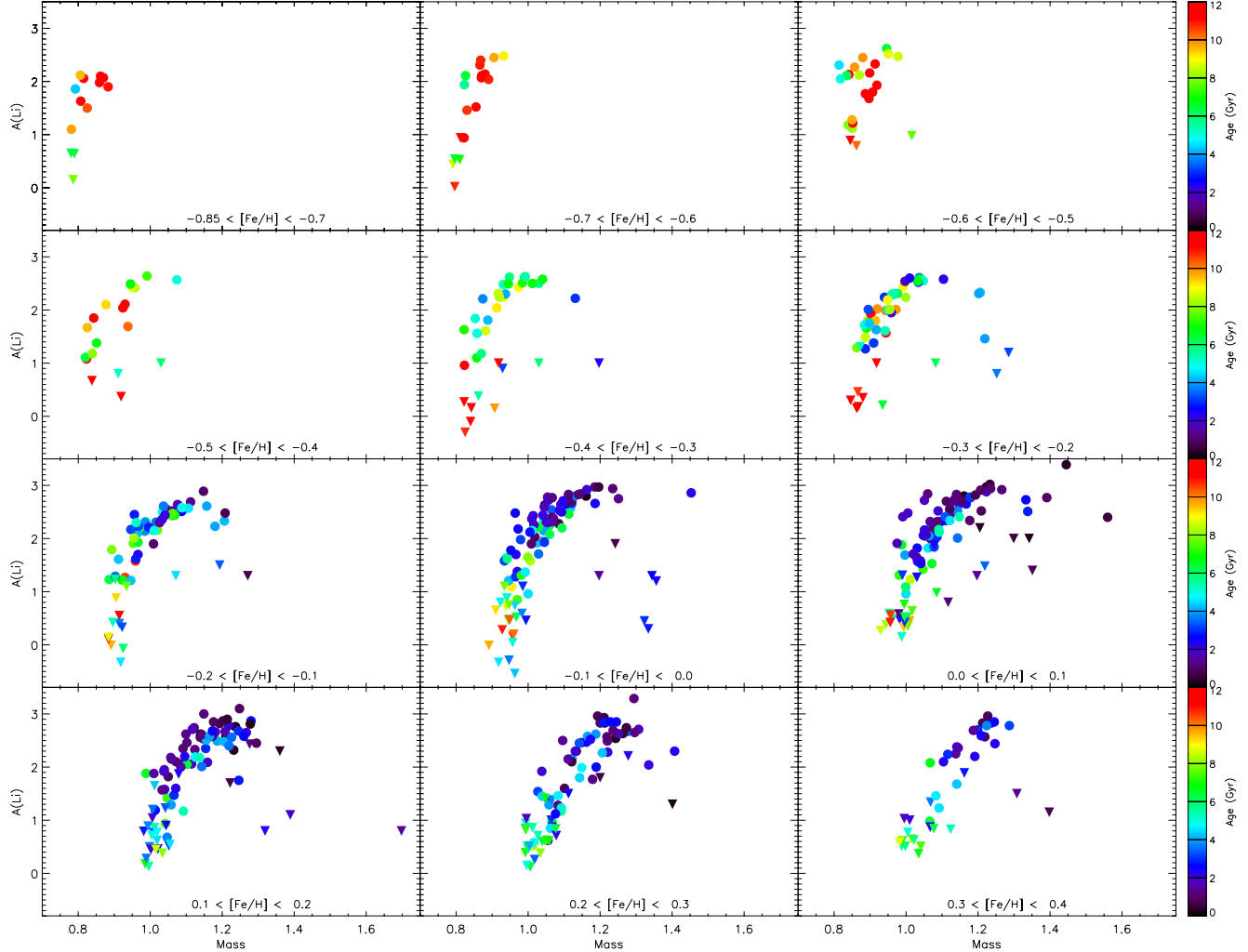


Fig. 3. Lithium abundances vs. stellar mass in 12 metallicity bins for all our stars with $\log g > 4.2$. Downward triangles represent $A(\text{Li})$ upper limits. The ages are depicted by a colour scale.

Finally, we investigate the possible effect of rotation on Li abundances for our sample of planet hosts. The models of rotationally-induced mixing predict that during the main sequence (MS), stars with higher rotation rates are expected to deplete more Li than slower rotators. We find that the average $v \sin i$ for hot jupiter hosts in this T_{eff} range is larger, 5 km s^{-1} (derived only for 11 stars) than for the comparison stars, 3.1 km s^{-1} (derived for 62 stars), hence this could explain the offset previously found for stars with hot jupiters. In order to test this effect, we repeat the same analysis as before except we include the $v \sin i$ in the equation and force a same dependence on it both for the planet host sample and in the comparison stars sample

$$\log(A(\text{Li})) = \text{int.} + \beta_1 \log(T_{\text{eff}}) + \beta_2 [\text{Fe}/\text{H}] + \beta_3 \log g + \beta_4 \log(\text{Age}) + \beta_5 v \sin i + M \times \text{offset.} \quad (2)$$

The results are shown in the second part of Table 1. As expected from the models of rotationally-induced mixing, Li abundances show a negative dependence on $v \sin i$. The offsets are now positive (i.e. higher Li abundances for planet hosts) but they are also much less significant than before (2.6σ and 2.1σ , for the jupiter size planets and the hot jupiters, respectively). This result points to an effect of rotation on Li abundances though we have to be cautious since our sample of measured $v \sin i$ values is very small and potentially biased (we could only measure $v \sin i$ in 42% of our stars with Li detections in this T_{eff} range).

3.3. The Li dip: dependence on metallicity, age and $v \sin i$

The Li dip was first discovered in the Hyades by Boesgaard & Tripicco (1986). For clusters younger than the Pleiades (~ 200 Myr) this feature is not observed and stars more massive than a solar mass show a constant maximum value of $A(\text{Li}) = 3\text{--}3.2$ dex (Lambert & Reddy 2004). Therefore, the Li dip has to be formed during the MS. Indeed, the maximum Li abundance is similar for the youngest clusters as for the slightly older clusters (300 Myr–2 Gyr), hence, F stars in the MS experience very little depletion up to ages of 1 Gyr. For older clusters there are hints of the presence of the dip though there is not always a significant number of stars at those temperatures. The Li dip is not well defined in Fig. 1 because in our sample there are stars of different ages and metallicities. To appreciate a clearly shaped Li dip one should divide the stars by ranges with similar [Fe/H] and age, as happens in open clusters.

In Fig. 3 we show Li abundances as a function of mass in 12 different metallicity bins for the stars in this work together with the sample of DM14 (we exclude the most metal-poor and most metal-rich bins due to their low number of stars). From this plot we can confirm that the Li dip happens at higher masses as the metallicity increases. This fact was first suggested by Balachandran (1995), who found that the mass at which the dip occurs depends on the stellar metallicity, while the zero age

main sequence (ZAMS) T_{eff} does not. Later studies on clusters (e.g. Cummings et al. 2012; François et al. 2013) or field stars (e.g. Lambert & Reddy 2004) have confirmed this feature. For example in the [Fe/H] range $[-0.6, -0.5]$, we have a unique star at the Li dip with a mass of $1.02 M_{\odot}$. This agrees with the Li dip centre of $1.06 M_{\odot}$ found by (François et al. 2013) in a similar metallicity cluster, NGC 2243 with [Fe/H] = -0.54 dex. By contrast, at higher metallicities we find two stars with 1.3 and $1.4 M_{\odot}$ in the Li dip, which compares well with the mass of the cool side of Li dip in NGC 6253 ($1.34 M_{\odot}$, [Fe/H] = 0.43 dex, Cummings et al. 2012). In that work they also compare their results with the Hyades, which has a Li dip mass of $1.27 M_{\odot}$. In our field stars of similar metallicity (0.1 – 0.2 dex), the Li dip seems to be at $\sim 1.3 M_{\odot}$. From Fig. 3 we can see that the increase of mass with metallicity not only happens for the Li dip stars but for all the objects within each metallicity bin, therefore this is just a reflection of the mass-metallicity correlation for stars with similar T_{eff} in the MS and confirms the suggestion by Balachandran (1995).

In Fig. 3 we also show the ages of the stars by a colour scale. For the more metal-poor bins we cannot observe the Li dip because our MS stars are too old and thus too cool to be susceptible to that process. For instance, for older clusters like M67 the Li dip is formed by subgiants. We have cleaned our sample of possible evolved stars so the hotter stars that usually form the Li dip have to be young enough and not evolved yet. In fact, if we observe the Li dip at different metallicities it is always formed by stars younger than ~ 4 Gyr, with the age slightly decreasing as the metallicity increases.

Several mechanisms have been proposed to explain the formation of the Li dip, such as mass loss (Schramm et al. 1990), diffusion, and radiative acceleration (Richer & Michaud 1993), or rotationally induced mixing (Zahn 1992; Pinsonneault et al. 1990). Under the assumption of this last mechanism, stars that rotate faster in the MS will experience more rapid mixing (thus, more Li depletion) than slow rotators at the same mass (Pinsonneault 1997). In principle, this seems to be at odds with the work by Bouvier (2008), where the slow rotators on the ZAMS suffer a stronger depletion of Li than fast rotators, and with the higher Li abundances found in rapidly rotating stars as compared with slow rotators of the same mass in the Pleiades (Soderblom et al. 1993; Garcia Lopez et al. 1994) or IC 2602 (Randich et al. 1997). However, at this point one has to be careful distinguishing between the depletion mechanisms acting during the MS and the PMS (e.g. Somers & Pinsonneault 2014) and between the current rotation rates and those in the ZAMS, though a priori one could expect that a star with a current high velocity was also a fast rotator in the past. Nevertheless, it is difficult to estimate the initial rotation velocity since stars usually spin down when arriving at the MS. Therefore we have to extract information from the current surface rotation rates. Moreover, for most of the stars, we do not know their inclination so we can only measure the projected rotational velocity, $v \sin i$, given that we have a good quality spectrum.

To check for the possible impact of rotation, we compare the $v \sin i$ values of the stars that typically form the Li gap (which we define in the range $6280 \text{ K} < T_{\text{eff}} < 6550 \text{ K}$, see Fig. 4). We note that in this plot the number of stars is lower since we were able to determine $v \sin i$ for only 20 out of 50 stars in this T_{eff} range. To increase the statistics we included 12 fast rotators within the same T_{eff} range analysed in Tsantaki et al. (2014), (see Table 2). For those stars the stellar parameters are derived using the spectral synthesis technique for FGK stars and are in agreement with the results of the EW method. In addition,

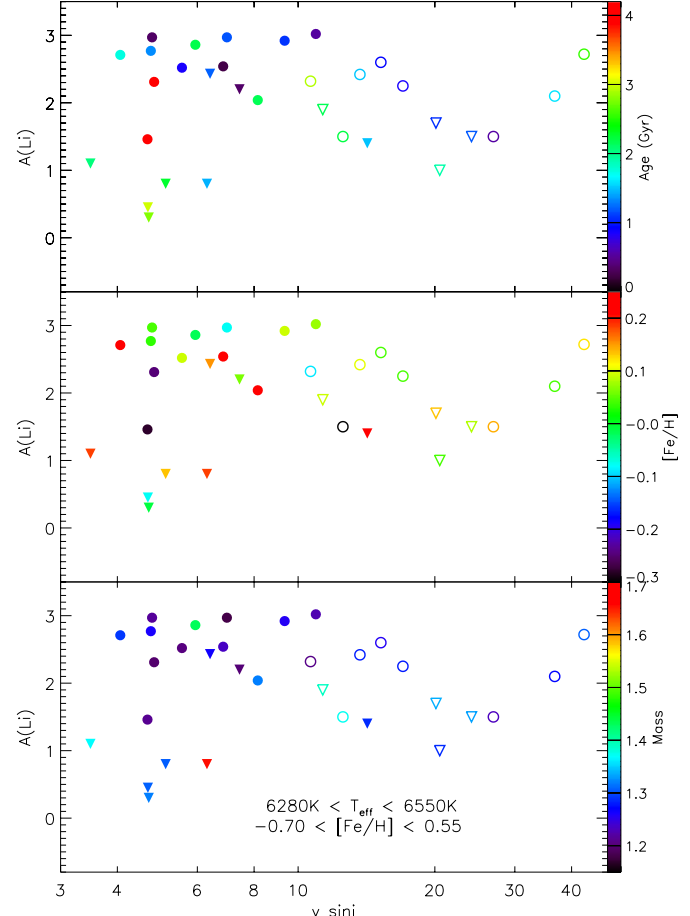


Fig. 4. Lithium abundances vs. $v \sin i$ around the Li dip for all our stars (filled circles and triangles). Open circles and triangles (upper limits) represent the fast rotators from Tsantaki et al. (2014). In each panel a colour scale shows the ages, metallicities, and masses of the stars.

the comparison of $v \sin i$ from the spectral synthesis technique mentioned above and our method shows a good agreement. The Li abundances for those 12 objects were derived in the same way as in this work. Therefore, the addition of the extra stars in Fig. 4 guarantees a uniform comparison.

We observe that the stars with the lowest Li abundances (< 1 dex) show low $v \sin i$ values (3 – 6 km s^{-1}) whereas the stars with the highest Li, which presumably surround the dip, present a wide range of rotation rates (~ 4 – 10 km s^{-1}). This could be caused by the fact that the dip stars are older on average than the stars with higher Li at the same $v \sin i$ (upper panel of Fig. 4). There seems to be a slight increase of the upper envelope of Li abundances with rotation up to 10 km s^{-1} , however, from that point Li abundances decrease sharply as the rotation increases. The fast rotators that form the upper envelope of Li abundances (within 10 – 30 km s^{-1}) have similar ages (< 1.5 Gyr) as the slower stars with high Li abundance. The lower panels of Fig. 4 illustrate that the metallicities and masses of both groups are comparable, thus we could expect that the higher rotation is producing extra depletion in these stars, as suggested by rotationally-induced mixing models. We could think then that, at young ages (< 1.5 Gyr), the Li dip is only formed by fast rotators, while for older ages the stars have had more time to deplete Li and to spin down at the same time, making it impossible to distinguish between rotationally induced mixing and other destruction mechanisms acting during the MS.

Table 2. Li abundances for the fast rotators of Sect. 3.3.

Star	T_{eff} (K)	$\log g$ (cm s^{-2})	[Fe/H]	Age (Gyr)	Mass (M_{\odot})	$v \sin i$ (km s^{-1})	$A(\text{Li})$
HD 142860	6361	4.07	-0.09	2.89	1.21	10.65	2.32
HD 89569	6469	4.08	0.09	2.14	1.41	11.33	<1.90
HD 86264	6300	4.06	0.25	2.19	1.39	12.55	1.50
HD 210302	6405	4.24	0.10	1.50	1.29	13.68	2.42
WASP-3	6423	4.42	0.04	0.93	1.27	15.21	2.60
HD 30652	6494	4.29	0.04	0.84	1.29	17.01	2.25
30AriB	6284	4.35	0.12	2.55	1.32	42.61	2.72
HAT-P-41	6479	4.39	0.13	1.05	1.35	20.11	<1.70
HAT-P-2	6414	4.18	0.04	1.91	1.30	20.50	<1.00
HAT-P-34	6509	4.24	0.08	1.17	1.35	24.08	<1.50
HD 8673	6472	4.27	0.14	0.55	1.24	26.91	1.50
CoRoT-11	6343	4.27	0.04	1.58	1.28	36.72	2.10

Notes. Stellar parameters from [Tsantaki et al. \(2014\)](#).

We checked whether the lack of stars with $v \sin i$ determination and Li upper limits could be biasing this effect. We could not determine $v \sin i$ values for nine stars (with Li upper limit), but only one out of those is young (WASP-32, 0.7 Gyr) and seems to be a slow rotator when we observe its spectrum. Thus, this is the only young star in our sample belonging to the dip with a low rotation rate. In any case, the small number of stars in this subsample suggests this result should be viewed with caution. Moreover, the rotational models predict a correlation between the rotation history of the star and Li depletion, rather than a correlation between the current rotation and the Li abundance ([Pinsonneault 1997](#)). There is another group of five fast rotators within the same $v \sin i$ range ($10\text{--}30 \text{ km s}^{-1}$), forming a lower envelope for Li abundances, probably related to their greater ages. We note that these are the only stars with $\log g < 4.2$ in Fig. 4 and we cannot rule out the possibility that they are subgiants. Curiously, for the two objects with the highest $v \sin i$ the trend changes, showing a higher Li abundance despite being older. We should consider this rise in Li abundance with caution since the determination of parameters becomes more difficult for the fastest rotators and the errors are three times larger than for the non-rotating counterparts.

3.4. Li evolution: dependence on [Fe/H] and age

To extract information about the evolution of Li through the life of the galaxy, it is very common to evaluate its behaviour with the metallicity. The well-known “Spite plateau” shows how the abundances of Li are nearly constant at $[\text{Fe}/\text{H}] \lesssim -1$ dex while they increase as $[\text{Fe}/\text{H}]$ increases. However, the available studies of clusters and field stars do not include very metal-rich stars with the exception of the recently analyzed cluster NGC 6253 ([Cummings et al. 2012](#)) with $[\text{Fe}/\text{H}] = 0.43$ dex. We note that a lower metallicity ($[\text{Fe}/\text{H}] = 0.23$ dex) has been obtained for this cluster by other authors ([Montalto et al. 2012](#)). Our sample of metal-rich planet hosts represents a good opportunity to check how the Li abundances behave at $[\text{Fe}/\text{H}] > 0.2$ dex.

In Fig. 5 we show the mean values of Li, stellar mass, T_{eff} , and age for the six stars with the highest Li abundance in each bin of metallicity. We chose this number of stars per bin to compare our results with the values obtained by [Lambert & Reddy \(2004\)](#) with a similar approach, who reported a good agreement with the maximum values found in open clusters of similar metallicity. We should consider the most metal-poor bins ($[\text{Fe}/\text{H}] < -0.7$ dex) with caution since we only have one or two

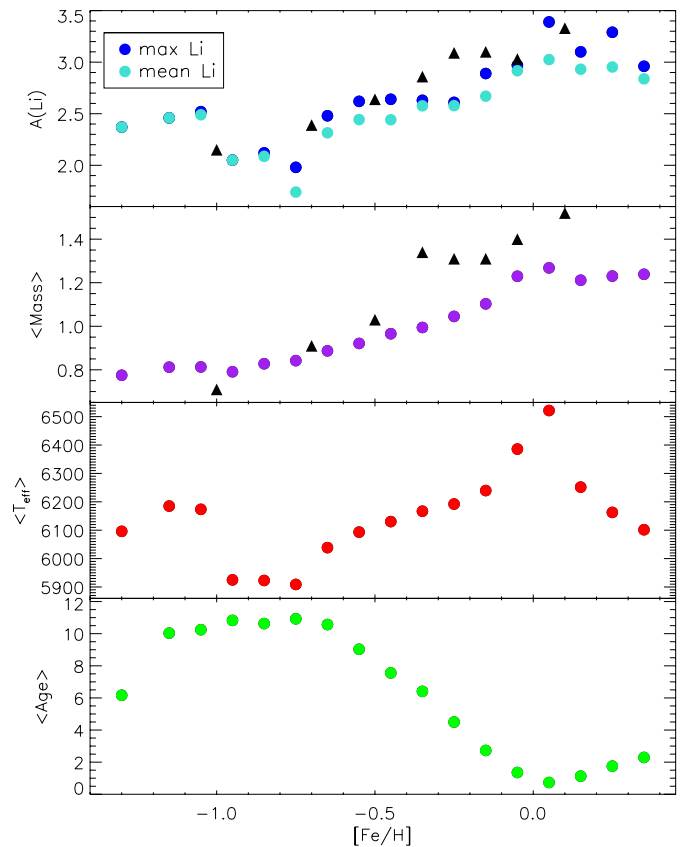


Fig. 5. Upper panel: maximum and mean values of Li in different metallicity bins for the six stars with the highest Li abundance in each metallicity bin (with $\log g > 4.2$). The circles are the values from this work and the triangles denote the values from [Lambert & Reddy \(2004\)](#). Remaining panels: mean values of mass, T_{eff} , and age for those six stars in each metallicity bin.

stars per bin and their temperatures fall out of the main trend. We compared our parameters with those derived by [Casagrande et al. \(2011\)](#) for these metal-poor stars and they agree well except for the most metal-poor star (HD 31128) for which [Casagrande et al. \(2011\)](#) gives a higher age, 8.26 Gyr.

For metallicities lower than solar, the Li abundance increases steadily with metallicity from a minimum at $[\text{Fe}/\text{H}] = -0.75$ dex with $A(\text{Li}) \sim 2$, close to the “Spite plateau”, up to $[\text{Fe}/\text{H}] \sim 0$ dex. Why the abundances increase from there up to the solar

metallicity? First, we can expect the more metallic stars to retain more of their initial Li because their masses are increasing (and thus the convective envelopes become shallower). Second, metal-rich stars are younger so they have less time to deplete their Li as observed in younger clusters (e.g. Sestito & Randich 2005). Finally, the models of Li production point to an increase of Li with time in the interstellar medium (e.g. Fields & Olive 1999; Prantzos 2012).

By contrast, for metallicities higher than solar, Li abundances seem to flatten and even decrease for the most metal-rich stars. As expected, the age decreases as [Fe/H] increases to reach a plateau for the most Li rich stars, where the age is between 1–2 Gyr. The maximum Li abundance, $A(\text{Li}) = 3.39$, is found at solar metallicity, which coincides with the minimum in age. We note here that this value corresponds to WASP-66, a very young and hot star ($T_{\text{eff}} = 7051$ K) compared with the average T_{eff} in our sample, hence the rise in average T_{eff} shown in the third panel of Fig. 5. That value also matches the maximum Li abundances found in young clusters such as NGC 2264 (Sestito & Randich 2005) and is very similar to the meteoritic abundance. Therefore it is possible that this represents the initial maximum Li abundance and those stars have not experienced any astration.

The standard model predicts that Li depletion is faster for more metallic stars since they have deeper convective zones. This is in contrast with the higher Li abundances found for the metal-rich stars. However, the models of Galactic Li production predict that initial Li abundance in a star becomes higher as the Galaxy evolves, i.e. as [Fe/H] increases. Indeed, the high Li abundances found in meteorites or in young clusters require Galactic production to increase the primordial Li abundance (either ~ 2.2 , from “Spite plateau” or ~ 2.7 from WMAP observations). The flattening observed at high [Fe/H] is possibly a balance between the higher initial Li in those stars (due to a larger content of Li in the interstellar medium), and a stronger destruction of Li due to the deepening of stellar convective zones. This possibility is suggested by the models of Fields & Olive (1999) who show that at super-solar metallicities the stellar Li depletion begins to affect the Li abundance in the inter-stellar medium, and thus flattening the correlation of initial Li and Fe. Therefore, in this scenario, we may think that the stars around solar metallicity represent the maximum Li in the Galaxy, which is similar to the initial value (and to the meteoritic value) since they are young and have not depleted it yet. As you move to super-solar metallicities the effect reverses and the high [Fe/H] begins to produce Li depletion. However, we should also note, as shown in Fig. 5, that the T_{eff} is also decreasing as [Fe/H] increases, therefore the convective envelope is getting deeper⁴ and probably affecting the depletion of Li.

The question remains how we can distinguish between a lower abundance of Li due to a lower initial abundance ([Fe/H] effect on Galactic production) or due to internal destruction during the MS (T_{eff} effect). In an attempt to disentangle both effects, we constructed samples of stars with different mass ranges but with $6000 \text{ K} < T_{\text{eff}} < 6200 \text{ K}$, as shown in Fig. 6. We chose this T_{eff} range because it is well populated with stars of different masses and metallicities. As expected, we cannot observe the stars with the highest Li abundance since we are not using the hottest stars. By restricting the sample, now the average T_{eff} , mass, and age of the stars are very similar in all the bins at

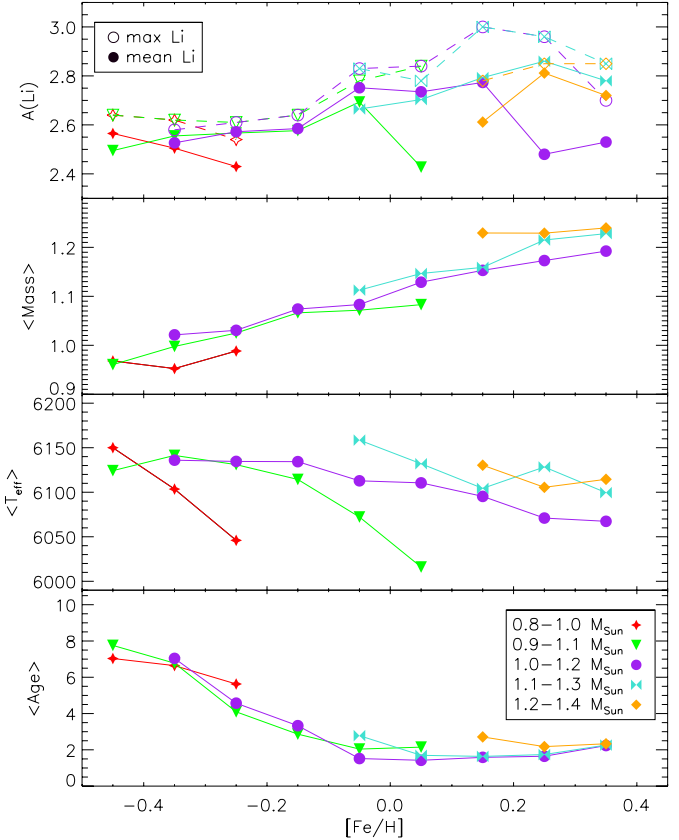


Fig. 6. Upper panel: maximum and mean values of Li in different metallicity bins for the six stars (when available) with the highest Li abundance in each metallicity bin (with $6000 \text{ K} < T_{\text{eff}} < 6200 \text{ K}$ and $\log g > 4.2$). Remaining panels: mean values of mass, T_{eff} , and age for those six stars in each metallicity bin.

super-solar metallicities, thus the observed variation of Li abundances should be triggered basically by the metallicity variation. We still observe the increase of Li with [Fe/H], with a maximum at $[Fe/H] = 0.15$ dex and a clear decrease for the subsamples between $1 M_{\odot}$ and $1.3 M_{\odot}$ (the most populated subsamples, designated by purple and blue symbols in Fig. 6). We evaluated the possible effect of planets on Li evolution, since as suggested before, planet hosts seem to have depleted more Li and our most metal-rich bins contain many of them. Thus, we reconstructed the samples between $1 M_{\odot}$ and $1.3 M_{\odot}$ with only comparison stars and we found that the behaviour is similar, i.e. Li decreases for the most metal-rich stars from $[Fe/H] \sim 0.15$ dex. Therefore, the lowest Li abundances found in the most metal-rich stars seem to be caused by a lower initial Li as predicted by some models of Galactic production (Fields & Olive 1999).

It is commonly accepted that Li abundances decrease with age, though the main depletion takes place principally during very young ages and depends on initial rotation rates (e.g. Charbonnel & Talon 2005) whereas after 1–2 Gyr the age effect is not so strong (Sestito & Randich 2005). In Fig. 7 we show the Li abundance as a function of age in four different T_{eff} bins. It is very clear that the higher abundances appear in the younger objects and then the Li upper envelope slightly decreases to reach a kind of a plateau. However we can still observe a high dispersion in Li for stars with similar T_{eff} , metallicity and age. For example, in the top-right panel, (6000 K–6100 K), for the most metallic stars ($[Fe/H] \sim 0.4$ dex, red symbols) there is a dispersion of ~ 0.8 dex in Li abundance determinations (not considering

⁴ Pinsonneault et al. (2001) show that T_{eff} is the main parameter determining the mass of convective envelopes with a very small effect of metallicity.

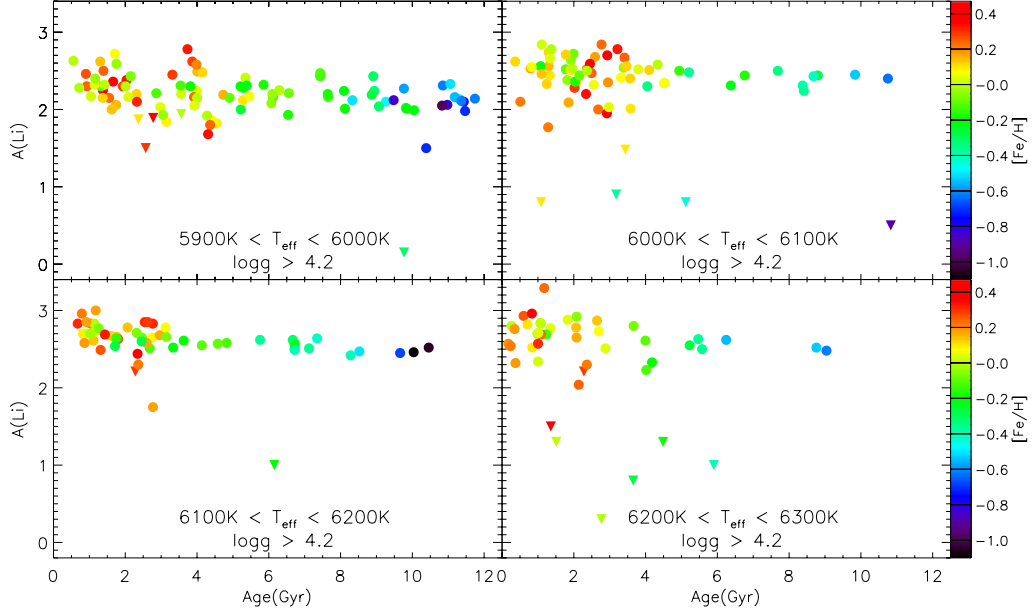


Fig. 7. Li abundances a function of age in several T_{eff} regions. The metallicity values are shown with a colour scale.

upper limits). For stars of solar metallicity (green points) the dispersion reaches 0.4 dex for stars of similar age. We find a similar spread in other T_{eff} and $[\text{Fe}/\text{H}]$ regions and the dispersion can reach values of 2 dex if we consider the upper limits. This fact reveals that an extra parameter is governing Li depletion. We may note here that when dealing with MS stars, the age determination is probably very uncertain (e.g. Jørgensen & Lindegren 2005), at least significantly more uncertain than other stellar parameters determination. Therefore, it might be possible that these stars of apparently same age could have quite different ages and that could be the reason of the spread in abundances. For instance, in clusters like the Hyades or NGC 6243 the spread around 6000 K is quite small (Cummings et al. 2012). In contrast, M67 or Praesepe show a huge dispersion in Li abundances (Sestito & Randich 2005).

3.5. Li in the Galactic disks

The recent work by Ramírez et al. (2012) presented a first attempt to compare Li abundances in the two Galactic disks. They found that the Li abundances for the thin disk stars (using a kinematical separation criteria) increase with metallicity, while for the thick disk stars the abundances have a nearly constant maximum value of $A(\text{Li}) \sim 2.1$ dex, similar to the “Spite plateau”. However, once they cleaned their thin disk sample of the youngest and more massive stars, to allow for a less biased comparison with the older and cooler thick disk, they found a smoother transition from the thick to the thin disk.

In Fig. 8 we present a plot, similar to Fig. 5. in Ramírez et al. (2012), using only the stars of the HARPS samples analyzed in Adibekyan et al. (2012). We note that we have removed planet hosts for this section since they only represent $\sim 10\%$ of the total sample and their abundances might be affected by the presence of planets (at least in the solar T_{eff} region). To improve the comparison we added a set of cool stars ($T_{\text{eff}} < 5600$ K) belonging to the HARPS samples (see Table 6). We used both kinematic⁵ and chemical criteria to separate the stellar populations

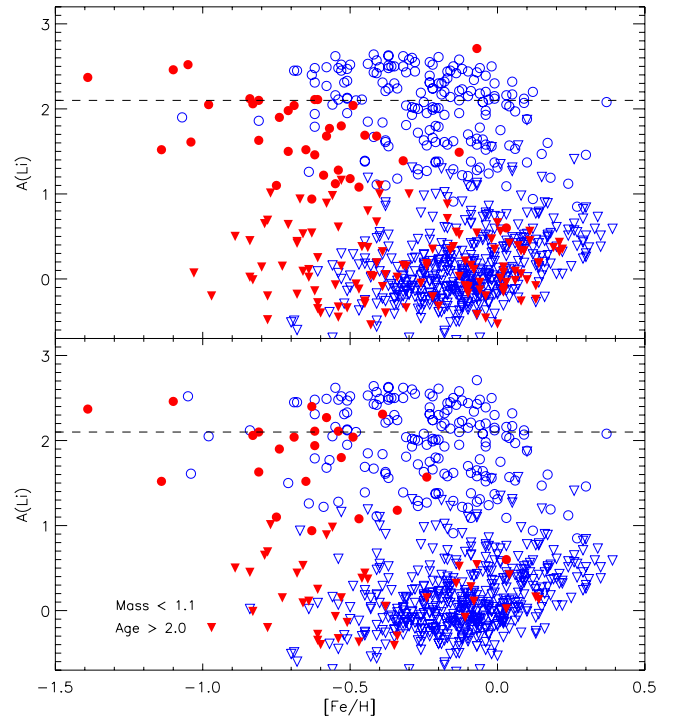


Fig. 8. Li abundances as a function of metallicity for the HARPS non-host stars. Thin disk stars are depicted with blue symbols while thick disk stars are denoted with red symbols. Downward triangles are upper limits on Li. The separation of the Galactic populations are based on the abundances (top) and kinematics (bottom). The constraint on age is only applied for the thin disk stars, as in Ramírez et al. (2012).

(see Adibekyan et al. 2011, 2012, for details). We note that stars with $[\text{Fe}/\text{H}] > -0.2$ dex and showing enhancement in α -element abundances were classified as members of a high- α metal-rich population in Adibekyan et al. (2011, 2013). Here we use the same symbol as for the thick disk stars to compare with the results of Ramírez et al. (2012) more easily.

Our thin disk stars also show slightly higher maximum abundances, decreasing for the more metal-rich stars as in the above

⁵ The kinematic separation was done using the prescription of Bensby et al. (2003) as presented in Adibekyan et al. (2012).

mentioned work and reflecting the evolution of Li at high metallicities discussed in the previous section. However, our thick disk stars also show a decrease of Li with metallicity from $[Fe/H] > -0.5$ dex, whereas in [Ramírez et al. \(2012\)](#) the thick disk stars present a constant value close to the “Spite plateau” up to $[Fe/H] \sim -0.1$ dex. Furthermore, this decrease seems steeper for the thick disk stars than for the thin disk stars. The lack of Li-rich metal-rich thick disk stars in our sample when compared to that observed in [Ramírez et al. \(2012\)](#) can probably be explained by the different criteria used to separate the stellar populations. However, both our kinematic and chemical separation shows the same picture. We should note that our kinematic criteria suggest very few thick disk stars with $[Fe/H] > -0.3$ dex, while in the sample of [Ramírez et al. \(2012\)](#) this metallicity region is quite abundant of thick disk stars. A more detailed analysis of their metal-rich Li-rich thick disk stars is needed to understand the nature of these stars and the reason for the observed discrepancy.

4. Summary

We present new Li abundances for a total sample of 36 planet hosts and 229 stars without detected giant planets in the HARPS GTO samples, together with 88 additional extrasolar planet hosts from other sources. All these stars span over an effective temperature range $5900 \text{ K} < T_{\text{eff}} < 7200 \text{ K}$. First, we find that planet hosts show an extra depletion of 0.07 dex in the T_{eff} range 5900–6300 K as previously claimed by [Gonzalez \(2015\)](#). This offset is statistically significant but close to the average uncertainties of Li abundances. However, this offset seems to be stronger for stars hosting hot jupiters (0.14 dex), something that could be explained by some models where the effect of planets on Li depletion is related with their mass and migration. This issue should be explored in the future with a larger sample of hot jupiters than the current sample of 24 stars analyzed here. In contrast, if we include the Li dependence on $v \sin i$ in our multivariate regression fit, the offset in Li abundance between the planet hosts and the comparison stars becomes positive but also decreases and becomes insignificant. This suggests that the difference in $v \sin i$ between both samples was causing the difference in Li abundances. Nevertheless, the number of stars for which we can derive $v \sin i$ is still too low to enable us to reach a conclusion regarding the effect of rotation on Li abundances for our sample of planet hosts.

We study the position of stellar mass of the Li dip at several metallicity bins. We confirm that the mass of the Li dip increases with the metallicity and extend this relation up to $[Fe/H] = 0.4$ dex. However, the mass of all the stars in our sample increases with metallicity, thus reflecting the mass-metallicity relation for dwarfs of the same temperature and supporting the idea of a constant T_{eff} for the Li dip. We also evaluate the behaviour of Li abundances with $v \sin i$ for the stars that surround the dip. We find that for the younger objects ($\lesssim 1.5$ Gyr), a strong depletion of Li only happens for fast rotators ($\gtrsim 10 \text{ km s}^{-1}$), suggesting that the Li dip is formed due to rotationally induced mixing at early stages of the MS. However, for the older objects the Li dip is formed by slower rotators, making it impossible to differentiate between the previously mentioned mechanism (we do not know if those stars were fast rotators at younger ages) or other depletion processes taking place during the MS.

Finally we analyze the Li evolution with the metallicity (i.e. the age of the Galaxy) since our metal-rich sample represents a good opportunity to check the behaviour of Li at super-solar

metallicities, which is not well studied in the literature. As expected from models of Galactic production of Li, we observe an increase of Li abundances as the Galaxy evolves, i.e. as the metallicity increases. We find the maximum abundance around $[Fe/H] \sim 0.1$ dex, with $A(\text{Li}) = 3.39$ dex, which is similar to the meteoritic value and the maximum Li abundances found in young clusters such as NGC 2264 ([Sestito & Randich 2005](#)). That said, Li abundances flatten and even decrease for the most metal-rich stars. This is in agreement with the models of [Fields & Olive \(1999\)](#) which suggest that the initial Li abundance of the most metal-rich stars is lower because the interstellar Li abundances have decreased due to the impact of stellar depletion during the evolution of the Galaxy. We also study the behaviour of Li in the context of thin and thick disks. We find a clear decrease of Li abundances at super-solar metallicities for the thin disk and a steeper decrease for thick disk stars that starts at $[Fe/H] > -0.5$ dex.

Acknowledgements. E.D.M., S.G.S. and V.Zh.A. acknowledge support from the Fundação para a Ciência e Tecnologia, FCT (Portugal) in the form of grants SFRH/BPD/7606/2011, SFRH/BPD/47611/2008, and SFRH/BPD/70574/2010, respectively. P.F. acknowledges support by Fundação para a Ciência e a Tecnologia (Portugal) through Investigador FCT contracts of reference IF/01037/2013 and POPH/FSE (EC) by FEDER funding through the program “Programa Operacional de Factores de Competitividade – COMPETE”. J.I.G.H. acknowledges support from the Spanish Ministry of Economy and Competitiveness (MINECO) under the 2011 Severo Ochoa Program MINECO SEV-2011-0187. N.C.S., A.M., and M.T. acknowledge support from the European Research Council/European Community under the FP7 through Starting Grant agreement number 239953, as well as support through programme Ciência 2007 funded by FCT/MCTES (Portugal) and POPH/FSE (EC), and in the form of grant PTDC/CTE-AST/098528/2008. A.M. is supported by the European Union Seventh Framework Programme (FP7/2007-2013) through grant agreement number 313014 (ETAEARTH). This research made use of the SIMBAD database operated at CDS, Strasbourg (France) and the Encyclopaedia of Extrasolar Planets. This work also made use of the IRAF facility.

References

- Adibekyan, V. Z., Santos, N. C., Sousa, S. G., & Israelian, G. 2011, [A&A, 535, L11](#)
- Adibekyan, V. Z., Sousa, S. G., Santos, N. C., et al. 2012, [A&A, 545, A32](#)
- Adibekyan, V. Z., Figueira, P., Santos, N. C., et al. 2013, [A&A, 554, A44](#)
- Alibert, Y., Mordasini, C., Benz, W., & Winisdoerffer, C. 2005, [A&A, 434, 343](#)
- Ammler-von Eiff, M., Santos, N. C., Sousa, S. G., et al. 2009, [A&A, 507, 523](#)
- Anders, E., & Grevesse, N. 1989, [Geochim. Cosmochim. Acta, 53, 197](#)
- Balachandran, S. 1995, [ApJ, 446, 203](#)
- Baumann, P., Ramírez, I., Meléndez, J., Asplund, M., & Lind, K. 2010, [A&A, 519, A87](#)
- Bensby, T., Feltzing, S., & Lundström, I. 2003, [A&A, 410, 527](#)
- Boesgaard, A. M., & Tripicco, M. J. 1986, [ApJ, 302, L49](#)
- Bonomo, A. S., Hébrard, G., Santerne, A., et al. 2012, [A&A, 538, A96](#)
- Bouvier, J. 2008, [A&A, 489, L53](#)
- Casagrande, L., Schöönrich, R., Asplund, M., et al. 2011, [A&A, 530, A138](#)
- Charbonnel, C., & Talon, S. 2005, [Science, 309, 2189](#)
- Chen, Y. Q., & Zhao, G. 2006, [AJ, 131, 1816](#)
- Chen, Y. Q., Nissen, P. E., Benoni, T., & Zhao, G. 2001, [A&A, 371, 943](#)
- Cummings, J. D., Deliyannis, C. P., Anthony-Twarog, B., Twarog, B., & Maderak, R. M. 2012, [AJ, 144, 137](#)
- da Silva, R., Udry, S., Bouchy, F., et al. 2007, [A&A, 473, 323](#)
- Delgado Mena, E., Israelian, G., González Hernández, J. I., et al. 2014, [A&A, 562, A92](#)
- Deliyannis, C. P., Demarque, P., & Kawaler, S. D. 1990, [ApJS, 73, 21](#)
- Fields, B. D., & Olive, K. A. 1999, [ApJ, 516, 797](#)
- Figueira, P., Faria, J. P., Delgado-Mena, E., et al. 2014, [A&A, 570, A21](#)
- François, P., Pasquini, L., Biazzo, K., Bonifacio, P., & Palsa, R. 2013, [A&A, 552, A136](#)
- García Lopez, R. J., Rebolo, R., & Martin, E. L. 1994, [A&A, 282, 518](#)
- Ghezzi, L., Cunha, K., Smith, V. V., & de la Reza, R. 2010, [ApJ, 724, 154](#)
- Gonzalez, G. 2008, [MNRAS, 386, 928](#)
- Gonzalez, G. 2014, [MNRAS, 441, 1201](#)

- Gonzalez, G. 2015, *MNRAS*, **446**, 1020
- Gonzalez, G., Carlson, M. K., & Tobin, R. W. 2010, *MNRAS*, **403**, 1368
- Israelian, G., Santos, N. C., Mayor, M., & Rebolo, R. 2004, *A&A*, **414**, 601
- Israelian, G., Delgado Mena, E., Santos, N. C., et al. 2009, *Nature*, **462**, 189
- Jørgensen, B. R., & Lindegren, L. 2005, *A&A*, **436**, 127
- Lambert, D. L., & Reddy, B. E. 2004, *MNRAS*, **349**, 757
- Lo Curto, G., Mayor, M., Benz, W., et al. 2010, *A&A*, **512**, A48
- Luck, R. E., & Heiter, U. 2006, *AJ*, **131**, 3069
- Mayor, M., Pepe, F., Queloz, D., et al. 2003, *The Messenger*, **114**, 20
- Molenda-Żakowicz, J., Sousa, S. G., Frasca, A., et al. 2013, *MNRAS*, **434**, 1422
- Montalto, M., Santos, N. C., Villanova, S., et al. 2012, *MNRAS*, **423**, 3039
- Mortier, A., Santos, N. C., Sousa, S. G., et al. 2013, *A&A*, **558**, A106
- Mortier, A., Sousa, S. G., Adibekyan, V. Z., Brandão, I. M., & Santos, N. C. 2014, *A&A*, **572**, A95
- Moutou, C., Loeillet, B., Bouchy, F., et al. 2006, *A&A*, **458**, 327
- Pinsonneault, M. 1997, *ARA&A*, **35**, 557
- Pinsonneault, M. H., Kawaler, S. D., & Demarque, P. 1990, *ApJS*, **74**, 501
- Pinsonneault, M. H., DePoy, D. L., & Coffee, M. 2001, *ApJ*, **556**, L59
- Pont, F., Tamuz, O., Udalski, A., et al. 2008, *A&A*, **487**, 749
- Prantzos, N. 2012, *A&A*, **542**, A67
- Ramírez, I., Fish, J. R., Lambert, D. L., & Allende Prieto, C. 2012, *ApJ*, **756**, 46
- Randich, S., Aharpour, N., Pallavicini, R., Prosser, C. F., & Stauffer, J. R. 1997, *A&A*, **323**, 86
- Richer, J., & Michaud, G. 1993, *ApJ*, **416**, 312
- Ryan, S. G. 2000, *MNRAS*, **316**, L35
- Santos, N. C., Israelian, G., & Mayor, M. 2004, *A&A*, **415**, 1153
- Santos, N. C., Israelian, G., Mayor, M., et al. 2005, *A&A*, **437**, 1127
- Santos, N. C., Ecuvillon, A., Israelian, G., et al. 2006, *A&A*, **458**, 997
- Santos, N. C., Mayor, M., Bonfils, X., et al. 2011, *A&A*, **526**, A112
- Santos, N. C., Sousa, S. G., Mortier, A., et al. 2013, *A&A*, **556**, A150
- Schramm, D. N., Steigman, G., & Dearborn, D. S. P. 1990, *ApJ*, **359**, L55
- Sestito, P., & Randich, S. 2005, *A&A*, **442**, 615
- Simón-Díaz, S., & Herrero, A. 2014, *A&A*, **562**, A135
- Soderblom, D. R., Jones, B. F., Balachandran, S., et al. 1993, *AJ*, **106**, 1059
- Somers, G., & Pinsonneault, M. H. 2014 [[arXiv:1410.4238](https://arxiv.org/abs/1410.4238)]
- Sousa, S. G., Santos, N. C., Israelian, G., Mayor, M., & Monteiro, M. J. P. F. G. 2006, *A&A*, **458**, 873
- Sousa, S. G., Santos, N. C., Mayor, M., et al. 2008, *A&A*, **487**, 373
- Sousa, S. G., Fernandes, J., Israelian, G., & Santos, N. C. 2010, *A&A*, **512**, L5
- Sousa, S. G., Santos, N. C., Israelian, G., et al. 2011a, *A&A*, **526**, A99
- Sousa, S. G., Santos, N. C., Israelian, G., Mayor, M., & Udry, S. 2011b, *A&A*, **533**, A141
- Takeda, Y., & Kawanomoto, S. 2005, *PASJ*, **57**, 45
- Takeda, Y., Honda, S., Kawanomoto, S., Ando, H., & Sakurai, T. 2010, *A&A*, **515**, A93
- Tsantaki, M., Sousa, S. G., Santos, N. C., et al. 2014, *A&A*, **570**, A80
- Udalski, A., Pont, F., Naef, D., et al. 2008, *A&A*, **482**, 299
- Zahn, J.-P. 1992, *A&A*, **265**, 115

Pages 11 to 24 are available in the electronic edition of the journal at <http://www.aanda.org>

Table 3. Li abundances for stars with planets from HARPS GTO samples.

Star	T_{eff} (K)	$\log g$ (cm s $^{-2}$)	ξ_t (km s $^{-1}$)	[Fe/H]	Age (Gyr)	Mass (M_{\odot})	A(Li)	Error	$v \sin i$ (km s $^{-1}$)	Hot jupiter
HD 142	6403	4.62	1.74	0.09	1.08	1.27	2.92	0.04	9.34	no
HD 10647	6218	4.62	1.22	0.00	0.26	1.16	2.80	0.03	5.30	no
HD 17051	6227	4.53	1.29	0.19	0.17	1.21	2.57	0.05	5.56	no
HD 19994	6289	4.48	1.72	0.24	2.14	1.34	2.04	0.07	8.15	no
HD 23079	5980	4.48	1.12	-0.12	6.12	1.00	2.16	0.04	2.96	no
HD 39091	6003	4.42	1.12	0.09	2.07	1.11	2.34	0.04	2.96	no
HD 52265	6136	4.36	1.32	0.21	1.04	1.20	2.83	0.05	-	no
HD 75289	6161	4.37	1.29	0.30	0.68	1.21	2.83	0.04	4.30	no
HD 82943	5989	4.43	1.10	0.26	0.90	1.15	2.46	0.04	2.75	no
HD 108147	6260	4.47	1.30	0.18	0.37	1.23	2.32	0.03	5.85	no
HD 117618	5990	4.41	1.13	0.03	4.00	1.08	2.24	0.03	3.67	no
HD 121504	6022	4.49	1.12	0.14	1.30	1.14	2.56	0.03	3.61	no
HD 169830	6361	4.21	1.56	0.18	2.04	1.39	<1.10	-	3.49	no
HD 179949	6287	4.54	1.36	0.21	0.24	1.24	2.54	0.04	6.84	yes
HD 196050	5917	4.32	1.21	0.23	3.91	1.12	2.16	0.03	3.34	no
HD 208487	6146	4.48	1.24	0.08	0.82	1.17	2.70	0.04	4.01	no
HD 209458	6118	4.50	1.21	0.03	1.19	1.13	2.73	0.05	-	yes
HD 212301	6271	4.55	1.29	0.18	0.35	1.24	2.76	0.04	5.76	yes
HD 213240	5982	4.27	1.25	0.14	4.01	1.19	2.49	0.05	3.50	no
HD 216435	6008	4.20	1.34	0.24	3.41	1.28	2.67	0.04	5.13	no
HD 221287	6374	4.62	1.29	0.04	0.33	1.22	2.97	0.04	4.77	no
HD 7449	6024	4.51	1.11	-0.11	1.77	1.06	2.52	0.03	3.51	no
HD 10180	5911	4.39	1.11	0.08	4.55	1.06	1.82	0.03	2.80	no
HD 93385	5977	4.42	1.14	0.02	3.56	1.07	2.20	0.03	2.99	no
HD 134060	5966	4.43	1.10	0.14	1.75	1.12	2.06	0.04	3.21	no
HARPS-4										
HD 190984	6007	4.02	1.58	-0.49	4.60	1.16	<0.50	-	3.23	no
HARPS-2										
HD 125612	5913	4.43	1.02	0.24	1.39	1.10	2.50	0.05	-	no
HD 145377	6054	4.53	1.11	0.12	1.25	1.12	2.33	0.04	3.76	no
HD 148156	6251	4.51	1.36	0.25	0.60	1.21	2.93	0.02	5.41	no
HD 153950	6074	4.39	1.23	-0.01	4.34	1.12	2.58	0.04	3.41	no
HD 156411	5910	3.99	1.31	-0.11	4.21	1.25	<0.30	-	3.34	no
HD 217786	5966	4.35	1.12	-0.14	7.65	1.02	2.16	0.07	-	no
HD 25171	6160	4.43	1.22	-0.11	4.13	1.09	2.55	0.06	-	no
HD 72659	5926	4.24	1.13	-0.02	6.29	1.06	2.25	0.07	-	no
HD 8535	6158	4.42	1.25	0.04	1.76	1.15	2.65	0.03	3.07	no
HD 9578	6055	4.52	1.07	0.11	1.30	1.12	2.74	0.04	2.36	no

Notes. Parameters from [Sousa et al. \(2008, 2011a,b\)](#).

Table 4. Li abundances for stars without detected planets from HARPS GTO samples.

Star	T_{eff} (K)	$\log g$ (cm s $^{-2}$)	ξ_t (km s $^{-1}$)	[Fe/H]	Age (Gyr)	Mass (M_{\odot})	A(Li)	Error	$v \sin i$ (km s $^{-1}$)
HD 361	5913	4.60	1.00	-0.12	1.33	1.03	2.30	0.05	2.96
HD 1388	5954	4.41	1.13	-0.01	4.00	1.04	2.15	0.03	3.18
HD 1581	5977	4.51	1.12	-0.18	5.86	0.99	2.32	0.02	3.03
HD 3823	6022	4.31	1.39	-0.28	8.80	0.99	2.44	0.03	3.00
HD 6735	6082	4.49	1.15	-0.06	1.92	1.09	2.64	0.04	3.71
HD 7134	5940	4.41	1.17	-0.29	9.82	0.92	2.02	0.05	2.71
HD 9782	6023	4.42	1.09	0.09	1.33	1.12	2.44	0.03	3.06
HD 11226	6098	4.35	1.28	0.04	3.79	1.14	2.52	0.03	3.03
HD 23456	6178	4.56	1.38	-0.32	6.67	0.99	2.62	0.04	3.20
HD 31822	6042	4.57	1.15	-0.19	1.07	1.04	2.56	0.04	3.77
HD 36108	5916	4.33	1.21	-0.21	9.84	0.97	2.01	0.05	2.95
HD 36379	6030	4.30	1.29	-0.17	6.76	1.07	2.44	0.04	2.98
HD 38382	6082	4.45	1.18	0.03	1.34	1.12	2.66	0.05	3.29
HD 38973	6016	4.42	1.14	0.05	2.56	1.10	2.32	0.04	3.29
HD 44120	6052	4.25	1.31	0.12	3.47	1.23	2.56	0.04	3.39
HD 44447	5999	4.37	1.26	-0.22	8.10	1.00	2.24	0.04	2.84

Notes. Parameters from [Sousa et al. \(2008, 2011a,b\)](#).

Table 4. continued.

Star	T_{eff} (K)	$\log g$ (cm s^{-2})	ξ_t (km s^{-1})	[Fe/H]	Age (Gyr)	Mass (M_{\odot})	$A(\text{Li})$	Error	$v \sin i$ (km s^{-1})
HD 55693	5914	4.43	1.07	0.29	2.57	1.11	<1.50	–	3.38
HD 65907A	5945	4.52	1.05	-0.31	9.77	0.91	<0.15	–	2.93
HD 68978A	5965	4.48	1.09	0.04	1.14	1.09	2.32	0.04	3.04
HD 69655	5961	4.44	1.15	-0.18	7.64	0.97	2.20	0.03	2.71
HD 70889	6051	4.49	1.13	0.11	0.37	1.14	2.62	0.03	3.45
HD 71479	6026	4.42	1.19	0.24	2.49	1.16	2.47	0.03	2.98
HD 73121	6091	4.30	1.34	0.09	3.44	1.22	<1.48	–	3.49
HD 73524	6017	4.43	1.14	0.16	0.79	1.15	2.53	0.03	3.15
HD 83529	5902	4.35	1.11	-0.22	10.05	0.94	1.99	0.04	2.47
HD 88742	5981	4.52	1.07	-0.02	0.72	1.09	2.28	0.03	2.45
HD 95456	6276	4.35	1.40	0.16	2.08	1.27	2.65	0.02	3.28
HD 105837	5907	4.54	1.14	-0.51	11.32	0.84	2.13	0.04	2.92
HD 119638	6069	4.42	1.22	-0.15	4.94	1.03	2.50	0.04	2.72
HD 122862	5982	4.23	1.29	-0.12	7.43	1.06	2.47	0.03	2.71
HD 125881	6036	4.49	1.10	0.06	0.82	1.12	2.55	0.03	2.94
HD 144585	5914	4.35	1.15	0.33	4.31	1.14	1.68	0.05	2.87
HD 145666	5958	4.53	1.04	-0.04	1.16	1.07	2.40	0.03	2.75
HD 157338	6027	4.44	1.17	-0.08	4.52	1.04	2.34	0.03	2.83
HD 162396	6090	4.27	1.43	-0.35	7.68	1.01	2.50	0.03	2.84
HD 168871	5983	4.42	1.17	-0.09	6.56	1.03	2.21	0.03	3.14
HD 171990	6045	4.14	1.40	0.06	3.47	1.29	2.77	0.02	3.06
HD 180409	6013	4.52	1.16	-0.17	2.04	1.03	2.36	0.05	3.43
HD 193193	5979	4.40	1.15	-0.05	6.07	1.06	2.08	0.03	3.19
HD 196800	6010	4.37	1.17	0.19	2.95	1.15	2.35	0.05	3.54
HD 199190	5926	4.26	1.14	0.15	4.73	1.12	2.19	0.03	2.69
HD 199960	5973	4.39	1.13	0.28	3.31	1.14	2.45	0.04	3.30
HD 204385	6033	4.44	1.15	0.07	3.31	1.11	2.41	0.04	3.63
HD 207129	5937	4.49	1.06	0.00	1.42	1.07	2.32	0.03	2.71
HD 220367	6128	4.37	1.34	-0.21	6.15	1.08	<1.00	–	3.48
HD 221356	6112	4.53	1.12	-0.20	3.63	1.04	2.61	0.03	3.69
<hr/>									
HARPS-4									
HD 25704	5942	4.52	1.37	-0.83	10.98	0.81	2.06	0.05	3.12
HD 31128	6096	4.90	3.02	-1.39	6.17	0.77	2.37	0.08	–
HD 38510	5914	4.32	1.30	-0.81	11.43	0.86	2.10	0.07	–
HD 59984	5962	4.18	1.45	-0.69	10.42	0.89	2.45	0.03	2.67
HD 61902	6209	4.38	1.58	-0.62	9.04	0.93	2.48	0.05	4.26
HD 68284	5933	4.08	1.40	-0.50	8.00	1.01	2.52	0.04	3.37
HD 88474	6122	3.91	1.91	-0.48	3.60	1.23	3.11	0.05	–
HD 90422	6085	4.14	1.67	-0.62	7.86	0.99	1.79	0.10	3.86
HD 94444	5998	4.34	1.29	-0.62	10.85	0.87	2.31	0.07	–
HD 95860	6054	4.48	1.25	-0.31	–	–	2.25	0.07	–
HD 102200	6185	4.59	1.52	-1.10	10.04	0.81	2.46	0.05	–
HD 109310	5922	4.55	1.15	-0.51	8.33	0.87	2.12	0.05	2.95
HD 109684	5992	4.38	1.22	-0.34	8.94	0.93	2.24	0.10	3.04
HD 119949	6359	4.47	1.65	-0.41	5.05	1.07	2.57	0.08	–
HD 123517	6082	4.08	1.53	0.09	–	–	1.94	0.10	5.81
HD 128340	6259	4.64	1.42	-0.55	6.24	0.95	2.62	0.07	–
HD 144589	6372	4.28	1.72	-0.05	–	–	1.82	0.10	–
HD 145344	6143	4.39	1.48	-0.68	9.66	0.90	2.45	0.06	–
HD 148816	5908	4.39	1.36	-0.71	11.47	0.86	1.98	0.07	2.70
HD 150177	6216	4.18	1.76	-0.58	7.29	1.02	2.49	0.02	3.84
HD 195633	6154	4.25	1.47	-0.51	8.52	0.98	2.47	0.06	3.95
HD 196892	6072	4.50	1.21	-0.89	10.83	0.83	<0.50	–	2.23
HD 197536	6105	4.39	1.34	-0.41	8.28	0.96	2.42	0.04	–
HD 210752	5951	4.53	1.20	-0.58	9.77	0.86	2.27	0.03	–
HD 215257	6052	4.46	1.40	-0.63	10.75	0.87	2.40	0.04	2.80
HD 218504	5962	4.34	1.21	-0.55	11.18	0.90	2.16	0.03	3.00
HD 223854	6080	4.08	1.60	-0.54	8.43	0.99	2.48	0.05	–
HD 224347	6092	4.27	1.31	-0.42	8.68	0.95	2.43	0.05	–
BD -084501	6216	4.81	2.36	-1.38	–	–	2.54	0.15	–
CD -231087	6788	4.67	1.82	-0.24	–	–	<1.00	–	5.37
CD -436810	6011	4.41	1.09	-0.44	5.12	0.91	<0.80	–	3.85
CD -451246	5960	4.42	0.75	-0.86	–	–	2.17	0.10	–
CD -571633	5975	4.46	1.14	-0.85	–	–	2.27	0.08	–

Table 4. continued.

Star	T_{eff} (K)	$\log g$ (cm s $^{-2}$)	ξ_t (km s $^{-1}$)	[Fe/H]	Age (Gyr)	Mass (M_{\odot})	A(Li)	Error	$v \sin i$ (km s $^{-1}$)
HARPS-2									
HD 101612	6281	4.41	1.17	-0.36	5.57	1.03	2.50	0.08	—
HD 102300	5987	4.23	1.14	-0.31	8.91	0.97	2.43	0.08	—
HD 103891	6072	4.05	1.50	-0.19	3.71	1.27	<0.10	—	3.69
HD 104760	5953	4.43	1.02	0.12	2.32	1.10	2.20	0.05	—
HD 105938	6208	4.27	1.60	0.03	2.88	1.34	2.51	0.06	—
HD 106290	6012	4.55	1.03	0.13	1.10	1.10	2.46	0.06	—
HD 108063	6081	4.11	1.54	0.55	2.06	1.58	<0.70	—	4.60
HD 111564	6004	4.37	1.13	0.07	4.51	1.12	2.34	0.07	—
HD 112283	6433	4.84	1.86	-0.13	0.94	1.15	2.89	0.08	—
HD 115341	6058	4.55	1.10	-0.01	1.95	1.09	2.53	0.06	—
HD 115773	6312	4.23	1.57	-0.08	2.99	1.32	<0.45	—	4.67
HD 116410	5939	4.43	1.07	0.23	1.55	1.11	2.15	0.05	—
HD 119629	6250	4.17	1.73	-0.17	3.25	1.30	<1.30	—	4.31
HD 123619	6166	4.45	1.38	-0.32	6.72	1.01	2.50	0.08	—
HD 123651	5926	4.55	1.05	-0.48	9.26	0.88	2.10	0.10	—
HD 126793	5910	4.46	1.26	-0.71	10.39	0.82	1.50	0.15	—
HD 128571	6159	4.40	1.23	-0.37	7.12	0.98	2.51	0.10	—
HD 129829	6196	4.66	1.30	-0.16	1.75	1.08	2.64	0.07	—
HD 130989	6414	4.27	1.85	-0.23	3.21	1.28	<1.20	—	—
HD 135468	6417	4.25	1.82	-0.02	2.17	1.45	2.86	0.07	5.94
HD 135625	6003	4.32	1.16	0.12	4.10	1.16	2.51	0.04	—
HD 139590	6200	4.49	1.31	0.13	2.06	1.22	2.78	0.05	—
HD 139879	6203	4.61	1.25	0.30	1.00	1.22	2.57	0.08	—
HD 141128	6758	4.67	1.65	0.07	0.32	1.34	<2.00	—	—
HD 141597	6285	4.38	1.23	-0.40	5.90	1.03	<1.00	—	—
HD 143638	5954	4.48	1.04	-0.27	5.22	0.95	2.00	0.08	2.84
HD 143790	6557	4.11	2.05	-0.06	1.80	1.56	2.90	0.06	5.43
HD 144846	6102	4.52	1.11	0.13	1.11	1.14	2.61	0.06	—
HD 144880	6152	4.38	1.33	-0.30	6.72	1.04	2.58	0.06	—
HD 14745	6290	4.72	1.46	-0.14	1.23	1.11	2.69	0.05	—
HD 148211	5922	4.34	1.31	-0.62	11.37	0.87	2.11	0.04	2.73
HD 149200	6416	4.64	1.74	0.15	0.96	1.29	2.45	0.09	—
HD 150139	5968	4.29	1.29	-0.51	11.06	0.91	2.33	0.04	—
HD 151772	6631	4.81	2.27	-0.36	3.02	1.13	2.22	0.15	—
HD 152433	6144	4.49	1.19	-0.10	4.58	1.11	2.57	0.05	—
HD 153276	6000	4.48	1.12	0.04	2.98	1.09	2.03	0.10	—
HD 154195	5961	4.48	1.01	-0.19	3.82	0.99	2.30	0.08	—
HD 156098	6517	4.20	2.06	0.18	1.44	1.70	<0.80	—	6.30
HD 156991	5934	4.57	0.99	-0.07	2.15	1.01	2.43	0.06	—
HD 160089	6312	4.78	1.60	0.11	0.67	1.20	2.87	0.08	—
HD 161566	6230	4.20	1.67	-0.28	3.66	1.25	<0.80	—	3.87
HD 163102	6433	4.64	1.94	0.00	1.13	1.24	2.94	0.06	—
HD 16382	5953	4.50	1.04	0.03	3.93	1.06	2.05	0.10	—
HD 173885	6264	4.37	1.61	-0.20	4.18	1.21	2.33	0.08	—
HD 174153	6196	4.49	1.34	-0.08	3.14	1.12	2.66	0.05	—
HD 17548	6011	4.44	1.18	-0.53	9.84	0.88	2.45	0.04	—
HD 176666	6103	4.63	1.18	-0.37	5.76	0.95	2.62	0.06	—
HD 177122	6021	4.52	1.03	-0.10	2.15	1.04	2.44	0.04	—
HD 179346	6229	4.76	1.35	-0.03	0.99	1.12	2.70	0.05	—
HD 18083	6144	4.70	1.33	0.03	0.96	1.11	2.70	0.05	—
HD 181428	6151	4.45	1.29	0.06	3.12	1.18	2.78	0.04	—
HD 188815	6217	4.34	1.31	-0.53	8.76	0.95	2.52	0.08	—
HD 191033	6206	4.47	1.35	-0.19	4.49	1.07	<1.30	—	—
HD 192865	6307	4.44	1.59	0.13	2.26	1.32	<0.80	—	5.11
HD 195200	6201	4.44	1.25	-0.08	3.67	1.13	2.80	0.05	—
HD 196384	6611	4.79	1.78	-0.13	0.77	1.21	2.48	0.15	—
HD 197300	6022	4.69	1.21	0.02	1.11	1.06	2.84	0.07	—
HD 199086	6149	4.65	1.21	0.18	0.86	1.17	2.58	0.05	—
HD 199289	5925	4.62	1.30	-0.98	10.83	0.79	2.05	0.08	—
HD 199868	6152	4.45	1.26	-0.13	4.82	1.09	2.58	0.05	—
HD 200538	6042	4.38	1.22	0.10	3.58	1.14	2.01	0.06	—
HD 201496	5974	4.44	1.12	-0.04	3.06	1.04	1.93	0.15	—
HD 202209	6009	4.68	1.19	-0.01	1.38	1.05	2.78	0.04	—
HD 202871	6055	4.54	1.04	-0.09	1.99	1.06	2.72	0.03	—

Table 4. continued.

Star	T_{eff} (K)	$\log g$ (cm s $^{-2}$)	ξ_t (km s $^{-1}$)	[Fe/H]	Age (Gyr)	Mass (M_{\odot})	$A(\text{Li})$	Error	$v \sin i$ (km s $^{-1}$)
HD 203335	6306	4.56	1.44	-0.04	2.42	1.19	2.66	0.05	—
HD 205294	6370	4.30	1.71	-0.25	4.01	1.20	2.31	0.05	4.82
HD 205591	6575	4.75	1.85	-0.08	1.38	1.25	2.75	0.06	7.68
HD 206116	6231	4.57	1.36	0.24	1.08	1.24	2.69	0.06	—
HD 207190	6182	4.33	1.51	-0.42	7.35	0.99	2.64	0.04	—
HD 208	5914	4.47	1.05	-0.31	9.07	0.91	2.04	0.04	2.59
HD 208068	6007	4.64	1.17	-0.38	3.18	0.93	<0.90	—	5.02
HD 20852	6813	4.76	2.34	-0.35	2.39	1.20	<1.00	—	6.08
HD 208672	5986	4.61	1.07	0.13	1.30	1.10	2.62	0.10	—
HD 211317	5965	4.30	1.21	0.27	3.87	1.19	2.62	0.05	—
HD 21132	6243	4.60	1.44	-0.37	5.47	0.99	2.63	0.03	3.11
HD 21161	5923	4.24	1.14	0.09	5.28	1.09	2.12	0.08	—
HD 214094	6288	4.28	1.46	-0.01	2.77	1.33	<0.30	—	4.69
HD 215625	6282	4.58	1.35	0.10	0.71	1.19	2.82	0.05	—
HD 215906	6259	4.56	1.55	-0.28	5.23	1.05	2.55	0.08	—
HD 217395	5916	4.52	0.95	-0.13	2.86	1.00	2.21	0.05	—
HD 217958	5970	4.45	1.29	0.28	1.93	1.13	2.30	0.15	—
HD 218379	5938	4.11	1.24	0.15	3.72	1.27	2.46	0.04	—
HD 21977	5930	4.45	1.03	0.10	2.37	1.08	<1.87	0.10	—
HD 220894	6282	4.60	1.35	0.02	1.00	1.18	2.34	0.05	—
HD 221638	6360	4.53	1.43	-0.21	2.23	1.10	2.58	0.08	—
HD 224578	6158	4.67	1.13	-0.01	1.14	1.11	2.83	0.07	—
HD 225297	6181	4.55	1.24	-0.09	2.46	1.11	2.65	0.05	—
HD 23030	5951	4.37	1.22	0.20	3.98	1.16	2.58	0.08	—
HD 24062	6107	4.62	1.34	0.28	2.63	1.23	2.85	0.05	—
HD 24085	6065	4.47	1.22	0.17	2.59	1.17	2.68	0.08	—
HD 24112	6175	4.35	1.26	0.16	2.60	1.26	2.58	0.05	3.10
HD 25587	6258	4.61	1.78	-0.12	4.02	1.18	2.23	0.15	—
HD 2567	6038	4.44	1.19	0.22	2.36	1.17	2.52	0.05	—
HD 25912	5900	4.52	0.99	0.12	1.37	1.06	2.15	0.06	—
HD 26887	6016	4.46	1.00	-0.35	4.05	0.94	2.30	0.07	—
HD 28969	6255	4.68	1.47	-0.01	1.07	1.15	2.84	0.06	—
HD 29980	6019	4.71	1.57	0.12	1.78	1.12	2.71	0.08	—
HD 30053	6139	4.51	1.20	-0.22	3.34	1.03	2.52	0.05	—
HD 31103	6078	4.49	1.08	0.09	1.09	1.12	<0.80	—	3.18
HD 3229	6583	4.14	1.80	-0.09	1.80	1.56	<2.00	—	—
HD 32804	5910	4.53	1.08	0.06	1.71	1.05	2.72	0.03	—
HD 33081	6399	4.56	2.47	-0.16	3.38	1.19	<1.50	—	—
HD 36051	6118	4.63	1.21	-0.08	1.26	1.07	2.77	0.05	—
HD 37226	6178	4.16	1.61	-0.12	2.77	1.39	<0.70	—	4.47
HD 37548	5950	4.26	1.19	-0.04	6.10	1.09	2.20	0.06	—
HD 37990	6215	4.56	1.15	0.00	1.08	1.14	2.83	0.05	—
HD 38385	7212	4.61	2.87	0.09	0.61	1.56	2.40	0.15	—
HD 38772	6106	4.37	1.16	-0.23	6.72	1.03	2.55	0.07	—
HD 40483	6371	4.39	1.80	-0.06	2.68	1.34	<1.30	—	—
HD 457	6089	4.43	1.17	0.34	2.45	1.21	2.59	0.04	—
HD 4597	6025	4.43	1.11	-0.39	8.38	0.92	2.31	0.08	—
HD 52449	6362	4.55	1.29	0.12	0.49	1.21	2.90	0.08	—
HD 5388	6311	4.24	1.65	-0.28	3.90	1.22	1.46	0.10	4.66
HD 54521	5973	4.54	1.02	-0.01	2.01	1.05	2.30	0.10	—
HD 564	5902	4.53	0.95	-0.20	5.21	0.96	2.30	0.04	2.44
HD 62364	6255	4.47	1.42	-0.11	3.99	1.16	2.61	0.06	—
HD 63754	6200	4.21	1.57	0.21	2.36	1.41	2.30	0.05	—
HD 65982	5947	4.42	1.08	-0.10	4.91	1.01	2.15	0.05	—
HD 66039	6149	4.52	1.14	0.17	0.92	1.18	2.85	0.04	—
HD 66168	6198	4.69	1.18	-0.03	1.03	1.11	2.70	0.06	—
HD 66740	6666	4.49	1.70	0.04	0.87	1.35	<1.40	—	—
HD 67200	6105	4.44	1.19	0.32	1.43	1.19	2.69	0.07	—
HD 68287	6318	4.63	1.45	0.06	0.95	1.21	2.91	0.05	—
HD 71685	6038	4.58	1.09	-0.37	5.21	0.93	2.48	0.05	—
HD 74957	5915	4.54	0.95	-0.18	6.54	0.97	1.93	0.08	3.07
HD 75328	6003	4.46	1.05	-0.23	6.38	0.98	2.31	0.08	—
HD 75881	6239	4.44	1.63	0.07	2.69	1.33	2.73	0.07	—
HD 76188	5989	4.08	1.25	-0.44	7.64	1.01	2.53	0.07	—
HD 82114	5912	4.20	1.28	0.01	5.35	1.15	2.41	0.05	—

Table 4. continued.

Star	T_{eff} (K)	$\log g$ (cm s $^{-2}$)	ξ_t (km s $^{-1}$)	[Fe/H]	Age (Gyr)	Mass (M_{\odot})	A(Li)	Error	$v \sin i$ (km s $^{-1}$)
HD 84305	5963	4.51	0.95	-0.23	5.39	0.97	2.31	0.07	—
HD 84627	6113	4.50	1.10	-0.28	1.71	1.00	2.54	0.06	—
HD 85725	5986	3.95	1.54	0.15	2.42	1.50	<0.56	—	5.85
HD 86652	5934	4.47	1.01	0.13	1.62	1.09	2.00	0.10	—
HD 87838	6118	4.47	1.33	-0.40	6.72	0.94	2.49	0.05	—
HD 8985	6473	4.96	2.15	-0.01	0.52	1.20	2.97	0.08	—
HD 90081	5912	4.34	1.08	-0.20	8.12	0.95	2.01	0.10	—
HD 90936	5928	4.48	1.04	0.03	2.08	1.05	2.16	0.08	—
HD 91379	6164	4.41	0.98	-0.29	2.46	1.01	2.60	0.10	—
HD 92547	6020	4.45	1.14	-0.37	8.41	0.92	2.24	0.08	—
HD 93745	6065	4.34	1.33	0.12	3.57	1.22	2.40	0.08	—
HD 93932	5950	4.30	1.16	0.05	5.46	1.09	2.17	0.07	—
HD 94964	6139	4.55	1.26	-0.07	2.32	1.10	2.71	0.05	—
HD 95542	5984	4.52	1.01	-0.04	1.75	1.04	2.59	0.03	—
HD 95922	6293	4.63	1.23	-0.06	2.08	1.16	2.92	0.05	—
HD 9608	5954	4.43	0.98	-0.26	8.87	0.95	2.19	0.05	—
HD 96276	6080	4.49	1.12	-0.02	2.37	1.09	2.50	0.05	—
HD 96290	6219	4.56	1.21	0.03	1.01	1.15	2.71	0.06	—
HD 97320	6162	4.57	1.50	-1.05	10.46	0.81	2.52	0.05	—
HD 98284	5913	4.52	1.18	-0.84	9.48	0.81	2.12	0.08	—
HD 131664	5901	4.50	1.04	0.31	2.32	1.10	2.10	0.04	3.01

Table 5. Li abundances for planet hosts not belonging to the HARPS-GTO sample.

Star	T_{eff} (K)	$\log g$ (cm s $^{-2}$)	ξ_t (km s $^{-1}$)	[Fe/H]	Age (Gyr)	Mass (M_{\odot})	A(Li)	Error	$v \sin i$ (km s $^{-1}$)	Hot jupiter	Flag	Ref.
HD 2039	5976	4.45	1.26	0.32	2.03	1.14	2.38	0.06	3.46	no	[1]	[c]
HD 8574	6151	4.51	1.45	0.06	2.75	1.17	2.65	0.10	—	no	[4]	[c]
HD 9826	6212	4.26	1.69	0.13	2.65	1.28	2.87	0.08	—	yes	[4]	[c]
HD 11506	6204	4.44	1.32	0.36	0.83	1.23	2.96	0.04	5.01	no	[1]	[b]
HD 13931	5940	4.42	1.19	0.08	3.15	1.08	1.84	0.15	—	no	[7]	[b]
HD 16175	6030	4.23	1.39	0.32	3.22	1.29	2.78	0.07	4.58	no	[9]	[b]
HD 17156	6084	4.33	1.47	0.23	2.77	1.21	2.84	0.05	—	no	[7]	[e]
HD 20367	6138	4.53	1.22	0.17	1.18	1.15	3.00	0.10	—	no	[10]	[c]
HD 23596	6108	4.25	1.30	0.31	2.77	1.24	2.83	0.05	—	no	[11]	[c]
HD 30562	5970	4.20	1.20	0.32	3.73	1.22	2.78	0.05	—	no	[3]	[d]
HD 31253	6147	4.27	1.47	0.17	2.77	1.25	1.75	0.07	3.25	no	[3]	[b]
HD 33283	6058	4.16	1.41	0.34	2.92	1.34	2.51	0.05	4.08	no	[1]	[b]
HD 34445	5915	4.30	1.11	0.24	4.36	1.14	1.80	0.08	—	no	[5]	[d]
HD 38283	5980	4.27	1.28	-0.14	7.43	1.06	2.43	0.05	3.80	no	[3]	[b]
HD 40979	6145	4.31	1.29	0.21	0.79	1.19	2.96	0.07	—	no	[4]	[c]
HD 43691	6200	4.28	1.49	0.28	2.28	1.28	<2.21	—	—	no	[7]	[i]
HD 50499	6056	4.29	1.23	0.39	2.93	1.20	2.70	0.07	—	no	[5]	[d]
HD 50554	6026	4.41	1.11	0.01	1.96	1.09	2.52	0.05	3.93	no	[11]	[c]
HD 60532	6273	4.02	1.88	-0.09	2.24	1.50	1.90	0.08	5.83	no	[2]	[b]
HD 68988	5988	4.45	1.25	0.36	1.38	1.14	2.25	0.10	—	no	[4]	[c]
HD 74156	6112	4.34	1.38	0.16	2.96	1.25	2.68	0.04	4.31	no	[3]	[c]
HD 75898	6137	4.31	1.36	0.30	2.54	1.25	2.85	0.06	4.32	no	[1]	[b]
HD 86081	6036	4.21	1.34	0.22	2.68	1.19	2.00	0.08	4.82	yes	[1]	[b]
HD 86226	5947	4.54	1.12	0.02	1.05	1.08	2.17	0.06	—	no	[3]	[b]
HD 86264	6596	4.47	1.90	0.37	0.81	1.40	<1.15	—	—	no	[3]	[b]
HD 89307	5967	4.51	1.33	-0.13	3.54	1.02	2.31	0.08	—	no	[4]	[d]
HD 95128	5954	4.44	1.30	0.06	4.44	1.07	1.85	0.15	—	no	[4]	[c]
HD 103774	6732	4.81	2.03	0.29	0.26	1.40	<1.30	—	7.95	no	[2]	[b]
HD 118203	5910	4.18	1.34	0.25	3.61	1.29	2.70	0.05	—	no	[4]	[b]
HD 120136	6339	4.19	1.70	0.23	1.49	1.30	<1.40	—	14.20	no	[1]	[c]
HD 142415	6045	4.53	1.12	0.21	0.51	1.12	2.10	0.10	—	no	[3]	[c]

Notes. The instrument used and the reference for the stellar parameters are shown in the last two columns. Flag: [1] UVES; [2] HARPS; [3] FEROS; [4] SARG; [5] CORALIE; [6] NOT; [7] SOPHIE; [8] HIRES; [9] FIES; [10] ELODIE; [11] UES.

References. [a] Mortier et al. (2013); [b] Santos et al. (2013); [c] Santos et al. (2004); [d] Sousa et al. (2006); [e] Ammler-von Eiff et al. (2009); [f] Santos et al. (2005); [g] Santos et al. (2006); [h] Moutou et al. (2006); [i] da Silva et al. (2007); [j] Molenda-Żakowicz et al. (2013); [k] Bonomo et al. (2012); [l] Pont et al. (2008); [m] Udalski et al. (2008).

Table 5. continued.

Star	T_{eff} (K)	$\log g$ (cm s $^{-2}$)	ξ_t (km s $^{-1}$)	[Fe/H]	Age (Gyr)	Mass (M_{\odot})	$A(\text{Li})$	Error	$v \sin i$ (km s $^{-1}$)	Hot jupiter	Flag	Ref.
HD 149026	6162	4.37	1.41	0.36	2.34	1.25	2.44	0.10	–	yes	[4]	[e]
HD 149143	6018	4.31	1.12	0.45	2.92	1.17	1.95	0.10	–	yes	[5]	[d]
HD 150706	5961	4.50	1.11	-0.01	0.56	1.05	2.63	0.04	–	no	[11]	[c]
HD 155358	5908	4.26	1.29	-0.62	11.74	0.88	2.14	0.10	3.12	no	[1]	[b]
HD 164509	5957	4.43	1.09	0.24	0.93	1.13	2.30	0.06	3.60	no	[2]	[b]
HD 176051	6030	4.68	1.28	-0.04	3.39	1.07	2.54	0.06	–	no	[7]	[b]
HD 183263	5991	4.38	1.23	0.34	1.66	1.14	2.36	0.05	–	no	[3]	[f]
HD 185269	5983	4.05	1.49	0.10	3.75	1.27	2.49	0.05	–	no	[10]	[h]
HD 187085	6146	4.36	1.31	0.13	1.76	1.18	2.66	0.06	3.74	no	[1]	[b]
HD 196067	5999	4.13	1.30	0.23	3.39	1.23	2.40	0.06	–	no	[3]	[b]
HD 196885A	6340	4.46	1.51	0.29	0.52	1.27	2.74	0.05	–	no	[4]	[d]
HD 205739	6301	4.40	1.42	0.21	1.74	1.31	2.71	0.04	4.06	no	[1]	[b]
HD 220689	5904	4.38	1.13	-0.01	4.28	1.03	1.92	0.06	–	no	[3]	[b]
HD 220773	5995	4.26	1.33	0.11	4.15	1.21	2.48	0.05	–	no	[3]	[b]
HD 224693	6053	4.18	1.40	0.28	3.00	1.32	2.09	0.08	4.20	no	[1]	[b]
HD 231701	6224	4.37	1.35	0.04	1.35	1.18	2.77	0.04	4.26	no	[1]	[b]
CoRoT-1	6397	4.66	1.68	0.03	0.95	1.39	2.77	0.06	4.74	no	[2]	[a]
CoRoT-4	6344	4.82	1.74	0.15	1.20	1.28	<2.43	–	6.40	no	[2]	[a]
CoRoT-5	6240	4.46	1.28	0.04	1.83	1.22	2.88	0.07	3.82	yes	[2]	[a]
HAT-P-1	6076	4.47	1.17	0.21	1.28	1.18	1.77	0.10	–	yes	[4]	[e]
HAT-P-4	6054	4.17	1.59	0.35	2.12	1.21	2.90	0.10	–	yes	[7]	[e]
HAT-P-6	6855	4.69	2.85	-0.08	0.73	1.24	<1.90	–	–	no	[7]	[e]
HAT-P-7	6525	4.09	1.78	0.31	1.05	1.42	3.29	0.10	–	no	[7]	[e]
HAT-P-8	6550	4.80	1.93	0.07	0.53	1.23	3.02	0.10	10.94	no	[9]	[a]
HAT-P-30	6338	4.52	1.40	0.12	0.85	1.25	3.10	0.06	–	no	[3]	[a]
HAT-P-35	6178	4.40	1.34	0.12	1.61	1.21	2.67	0.05	–	yes	[3]	[a]
Kepler-21	6409	4.43	1.86	-0.03	2.42	1.36	<1.20	–	–	no	[7]	[j]
Kepler-43	6041	4.26	1.85	0.33	2.34	1.19	2.20	0.15	–	yes	[7]	[k]
OGLE-TR-10	6075	4.54	1.45	0.28	2.02	1.22	2.28	0.10	6.43	yes	[1]	[g]
OGLE-TR-182	5924	4.47	0.91	0.37	2.78	1.16	<1.89	–	4.53	no	[1]	[l]
OGLE-TR-211	6325	4.22	1.63	0.11	–	–	<1.50	–	7.10	no	[1]	[m]
OGLE-TR-56	6119	4.21	1.48	0.25	1.80	1.25	2.63	0.10	5.25	yes	[1]	[g]
TrES-4	6293	4.20	2.01	0.34	1.36	1.31	<1.50	–	–	no	[7]	[e]
WASP-1	6252	4.32	1.42	0.23	1.17	1.29	3.29	0.08	3.66	yes	[1]	[a]
WASP-7	6621	4.62	3.00	0.12	0.71	1.22	<1.70	–	17.48	no	[1]	[a]
WASP-12	6313	4.37	1.65	0.21	1.18	1.30	2.65	0.08	–	no	[3]	[a]
WASP-13	6025	4.19	1.28	0.11	2.93	1.16	2.17	0.08	4.35	yes	[8]	[a]
WASP-15	6573	4.79	1.72	0.09	0.52	1.30	<2.00	–	4.77	no	[2]	[a]
WASP-17	6794	4.83	2.57	-0.12	0.74	1.27	<1.30	–	8.87	no	[2]	[a]
WASP-18	6526	4.73	1.83	0.19	0.33	1.28	2.81	0.10	–	no	[3]	[a]
WASP-21	5924	4.39	1.06	-0.22	5.29	0.96	2.28	0.10	–	yes	[3]	[a]
WASP-22	6153	4.57	1.36	0.26	1.31	1.22	2.49	0.10	4.29	yes	[2]	[a]
WASP-24	6297	4.76	1.41	0.09	0.84	1.21	2.52	0.08	5.55	yes	[2]	[a]
WASP-26	6034	4.44	1.28	0.16	1.85	1.16	2.09	0.10	–	yes	[3]	[a]
WASP-28	6134	4.55	1.17	-0.12	2.68	1.09	2.51	0.10	4.39	yes	[2]	[a]
WASP-31	6443	4.76	1.62	-0.08	1.16	1.18	2.97	0.08	6.97	no	[2]	[a]
WASP-32	6427	4.93	1.20	0.28	0.73	1.20	<1.80	–	–	no	[3]	[a]
WASP-35	6072	4.69	1.26	-0.05	1.82	1.07	2.38	0.08	–	yes	[3]	[a]
WASP-36	5928	4.51	0.89	-0.01	3.56	1.05	<1.94	–	4.01	no	[2]	[a]
WASP-38	6436	4.80	1.75	0.06	0.35	1.21	<2.20	–	7.43	no	[2]	[a]
WASP-54	6296	4.37	1.45	0.00	1.51	1.20	<1.30	–	–	no	[3]	[a]
WASP-55	6070	4.55	1.10	0.09	1.90	1.14	2.51	0.08	–	yes	[3]	[a]
WASP-62	6391	4.73	1.50	0.24	0.50	1.26	2.63	0.06	–	no	[3]	[a]
WASP-66	7051	5.00	3.07	0.05	0.38	1.45	3.39	0.06	–	no	[3]	[a]
WASP-71	6180	4.15	1.69	0.37	1.68	1.27	2.33	0.10	–	yes	[3]	[a]
WASP-78	6291	4.19	1.63	-0.07	2.21	1.19	<1.50	–	–	no	[3]	[a]
WASP-79	7002	4.77	2.64	0.19	0.39	1.36	<2.30	–	–	no	[3]	[a]

Table 6. Li abundances for cool stars without detected planets from HARPS GTO samples.

Star	T_{eff} (K)	$\log g$ (cm s $^{-2}$)	ξ_t (km s $^{-1}$)	[Fe/H]	Age (Gyr)	Mass (M_{\odot})	$A(\text{Li})$
HD 100289	5483	4.42	0.70	0.03	4.09	0.92	<0.35
HD 102136	5349	4.43	0.75	-0.09	3.92	0.86	<0.00
HD 102843	5432	4.35	0.79	0.16	3.04	0.92	<-0.21
HD 103720	5017	4.43	0.90	-0.02	4.00	0.79	<-0.51
HD 106589	5597	4.37	0.67	-0.23	6.83	0.88	<0.53
HD 107094	5564	4.54	0.75	-0.51	5.28	0.81	1.95
HD 108341	5122	4.45	0.64	0.04	4.70	0.84	<-0.21
HD 109988	5193	4.46	0.81	0.14	5.06	0.88	<0.15
HD 110291	5480	4.38	0.69	-0.02	4.17	0.90	<0.31
HD 110557	5267	4.36	0.71	-0.06	4.07	0.84	<-0.69
HD 112100	5081	4.44	0.50	-0.16	4.39	0.79	<-0.51
HD 113569	4994	4.41	0.41	-0.22	4.58	0.76	<-0.20
HD 114076	5069	4.32	0.04	-0.47	5.56	0.74	<-0.37
HD 115499	5542	4.45	0.95	0.07	3.51	0.94	<1.57
HD 11608	4959	4.32	0.56	0.22	4.28	0.82	<0.06
HD 116883	4902	4.36	0.52	-0.20	4.75	0.75	<-0.28
HD 1171	5293	4.47	0.48	-0.53	4.18	0.75	<0.00
HD 117359	5246	4.43	0.68	-0.13	4.90	0.83	<-1.02
HD 118466	5049	4.34	0.49	0.20	4.93	0.86	<0.06
HD 118563	5477	4.45	0.68	-0.04	3.59	0.89	<0.23
HD 119503	4885	4.40	0.83	-0.04	4.37	0.77	<-0.07
HD 120362	5517	4.51	1.05	0.10	2.68	0.93	<0.78
HD 122308	5253	4.44	0.59	-0.32	4.35	0.78	<0.04
HD 125522	4839	4.45	0.40	-0.46	4.39	0.70	<-0.30
HD 127124	5079	4.43	0.82	-0.04	4.84	0.82	<-0.37
HD 128113	4922	4.28	0.35	-0.17	5.01	0.77	<-0.32
HD 128431	5429	4.43	0.61	-0.34	5.01	0.82	<0.14
HD 13252	5358	4.33	0.59	-0.25	4.63	0.83	<0.11
HD 132569	5026	4.49	0.59	-0.26	4.29	0.75	<-0.37
HD 133633	5571	4.48	0.69	-0.45	7.13	0.82	<0.24
HD 134929	5330	4.36	0.79	0.07	4.70	0.90	<-0.22
HD 138799	5224	4.36	0.71	0.02	5.26	0.87	<0.38
HD 138914	4983	4.38	0.66	-0.12	4.81	0.78	<-0.32
HD 139710	5123	4.41	0.90	-0.08	4.09	0.81	<0.02
HD 141598	5593	4.37	0.75	-0.10	6.19	0.91	<0.20
HD 144342	5403	4.47	0.90	0.07	4.09	0.90	<-0.07
HD 147195	5557	4.48	0.68	-0.05	6.05	0.92	<0.49
HD 150474	5425	4.01	0.96	0.01	7.60	1.09	1.75
HD 155717	4949	4.48	0.76	-0.13	3.96	0.76	<-0.37
HD 15612	5256	4.49	0.87	-0.11	4.17	0.83	<-1.01
HD 156423	5184	4.46	0.21	-0.43	4.76	0.75	<0.15
HD 156517	5013	4.45	0.81	0.03	4.41	0.81	<0.03
HD 157668	5195	4.49	0.65	-0.23	4.48	0.79	<-0.03
HD 15906	4884	4.49	0.65	-0.01	4.33	0.78	<-0.41
HD 16536	5282	4.39	0.70	-0.08	4.57	0.85	<0.23
HD 168769	5361	4.45	0.87	-0.01	3.62	0.87	<0.26
HD 168870	5325	4.43	0.67	-0.32	4.89	0.81	<-0.15
HD 170958	5599	4.83	1.38	-0.04	3.05	0.91	2.39
HD 171825	4908	4.48	0.39	-0.12	4.25	0.76	<-0.34
HD 177033	4918	4.50	0.45	-0.13	3.95	0.75	<-0.15
HD 181249	4906	4.25	0.24	-0.13	4.90	0.77	<-0.42
HD 18777	5058	4.39	0.57	0.01	4.43	0.82	<0.00
HD 188091	5120	4.32	0.87	0.08	4.53	0.85	<0.29
HD 18822	5272	4.43	0.87	-0.07	4.79	0.85	<1.13
HD 18838	5500	4.48	0.64	-0.17	4.16	0.87	<0.10
HD 189004	5094	4.36	0.67	-0.07	5.27	0.82	<-0.11
HD 190204	5476	4.63	1.14	-0.02	4.30	0.90	<1.55
HD 191797	5061	4.50	0.86	-0.06	4.82	0.81	1.31
HD 19230	5254	4.63	0.46	-0.57	4.59	0.74	<-0.39
HD 194717	5247	4.26	0.33	-0.28	5.71	0.81	<0.25
HD 196397	5378	4.33	0.68	0.29	4.08	0.93	<0.24
HD 200143	5112	4.46	0.96	0.02	4.44	0.83	<-0.13
HD 201161	4884	4.36	0.63	-0.04	4.11	0.76	<-0.22

Notes. Parameters from Sousa et al. (2008, 2011a,b).

Table 6. continued.

Star	T_{eff} (K)	$\log g$ (cm s^{-2})	ξ_t (km s^{-1})	[Fe/H]	Age (Gyr)	Mass (M_{\odot})	$A(\text{Li})$
HD 2014	5054	4.37	0.64	-0.07	4.43	0.80	<-0.16
HD 203771	4963	4.43	0.50	0.13	4.23	0.81	<-0.27
HD 203897	5184	4.42	0.65	-0.18	4.14	0.80	<-0.61
HD 206630	4853	4.48	0.06	-0.41	4.44	0.70	<-0.49
HD 209566	5500	4.38	0.75	0.12	4.86	0.94	<0.37
HD 210329	4965	4.40	0.45	-0.18	5.05	0.77	<-0.35
HD 210507	4998	4.42	0.69	0.07	4.42	0.82	<0.04
HD 211188	5053	4.41	0.42	-0.12	4.29	0.79	<0.11
HD 211534	5032	4.43	0.14	-0.31	4.34	0.74	<-0.11
HD 21251	4920	4.41	0.68	-0.09	4.99	0.78	<-0.06
HD 212918	5051	4.48	0.41	-0.21	4.30	0.77	<-0.20
HD 213852	4943	4.24	0.40	0.15	4.59	0.83	<0.27
HD 215902	5454	4.46	0.53	-0.25	4.24	0.84	<0.29
HD 216215	5220	4.45	0.58	-0.20	4.07	0.80	<0.34
HD 217221	5184	4.45	0.77	0.01	4.46	0.85	<-0.09
HD 21759	5142	4.49	0.43	-0.61	4.52	0.72	<0.09
HD 221974	5170	4.30	0.74	0.30	4.51	0.88	<0.30
HD 222721	5361	4.43	0.52	-0.31	5.13	0.82	<0.16
HD 22282	5433	4.32	0.77	0.12	7.18	0.93	<0.59
HD 224047	5167	4.43	0.62	-0.23	4.89	0.79	<-0.02
HD 224230	4944	4.47	0.56	-0.10	4.07	0.76	<-0.29
HD 224287	5330	4.38	0.59	-0.29	4.37	0.81	<-0.02
HD 224433	5527	4.42	0.72	0.09	3.37	0.94	<0.19
HD 224685	5504	4.47	0.76	-0.40	4.64	0.81	<0.50
HD 24558	5274	4.40	0.67	-0.47	5.48	0.77	<0.17
HD 25061	5243	4.42	0.80	0.07	5.76	0.88	<0.21
HD 25357	5117	4.72	1.02	-0.03	3.48	0.80	<0.04
HD 26430	4948	4.37	0.55	-0.26	4.91	0.75	<-0.46
HD 2768	5548	4.40	0.81	-0.03	3.79	0.92	<0.76
HD 290038	5006	4.42	0.56	0.01	4.64	0.81	<0.00
HD 30669	5400	4.37	0.55	0.13	4.69	0.92	<0.46
HD 30858	5182	4.45	0.88	-0.13	4.59	0.81	<0.19
HD 309701	4814	4.39	0.00	-0.30	4.47	0.71	<-0.69
HD 323631	4984	4.44	0.38	-0.28	4.45	0.74	<-0.21
HD 33811	5554	4.39	0.78	0.30	4.39	0.98	<0.26
HD 36179	5327	4.45	0.69	-0.08	3.77	0.85	<0.40
HD 3808	5572	4.46	0.82	-0.17	5.63	0.89	<0.96
HD 38265	5549	4.43	0.72	-0.14	5.69	0.90	<0.59
HD 38355	5314	4.35	0.75	0.09	4.91	0.89	<0.43
HD 40503	4953	4.29	0.81	-0.03	4.93	0.80	<0.02
HD 41087	5562	4.52	0.85	-0.13	4.37	0.90	1.95
HD 4457	5015	4.53	0.65	-0.37	4.82	0.74	<-0.08
HD 44804	5366	4.48	0.97	0.03	4.40	0.89	<0.11
HD 58676	5104	4.37	0.75	-0.02	4.67	0.83	<0.36
HD 62847	5362	4.48	0.67	-0.25	3.94	0.82	<0.16
HD 64640	5174	4.31	0.77	0.18	4.72	0.88	<0.18
HD 66040	5226	4.34	0.76	0.35	4.43	0.89	<0.38
HD 66340	5284	4.36	0.75	0.03	4.02	0.87	<-0.02
HD 66838	5392	4.29	0.71	0.03	4.32	0.89	<0.45
HD 70903	5118	4.52	0.63	-0.43	5.29	0.75	<0.02
HD 78964	5195	4.50	0.91	0.10	4.65	0.87	1.37
HD 81767	4978	4.46	0.68	0.05	4.62	0.82	<-0.13
HD 88885	5361	4.46	0.77	-0.11	4.59	0.86	<0.69
HD 89147	5310	4.45	0.76	-0.09	3.91	0.85	<0.42
HD 89749	5443	4.48	0.61	-0.29	5.17	0.83	<0.24
HD 89920	4827	4.32	0.10	-0.03	5.02	0.78	<-0.27
HD 89965	5039	4.48	0.72	-0.09	4.45	0.79	<0.02
HD 90133	5064	4.42	0.37	-0.16	5.07	0.79	<0.27
HD 90926	5538	4.35	0.80	0.13	5.20	0.95	<0.25
HD 91267	4928	4.48	0.26	-0.06	4.73	0.79	<-0.19
HD 93351	5408	4.41	0.57	-0.23	5.24	0.85	<0.21
HD 95533	5366	4.36	0.63	0.16	4.37	0.92	<0.20
BD -050578	5470	4.39	0.79	0.09	2.88	0.91	<0.40
BD -054065	4895	4.41	0.42	-0.29	4.36	0.72	<-0.11
BD -060904	5066	4.46	0.46	-0.17	4.05	0.77	<0.10

Table 6. continued.

Star	T_{eff} (K)	$\log g$ (cm s^{-2})	ξ_t (km s^{-1})	[Fe/H]	Age (Gyr)	Mass (M_{\odot})	$A(\text{Li})$
BD -112763	4911	4.44	0.38	-0.26	3.92	0.72	<-0.30
BD -131161	5389	4.37	0.68	0.09	4.00	0.90	<0.35
BD -160308	5183	4.48	0.51	-0.41	4.55	0.75	<0.18
BD -160931	4840	4.38	0.46	-0.11	4.58	0.75	<-0.25
HIP 10741	4859	4.40	0.51	-0.15	3.89	0.73	<-0.12
HIP 116939	4984	4.35	0.56	-0.07	4.82	0.79	<0.43
HIP 12147	5050	4.50	0.43	-0.32	4.84	0.75	<-0.20
HIP 15587	5239	4.46	0.66	-0.12	3.63	0.81	<0.06
HIP 16094	4877	4.44	0.39	-0.04	4.04	0.76	<0.06
HIP 1745	5416	4.39	0.47	-0.44	4.47	0.79	<1.19
HIP 20444	4907	4.41	0.54	-0.12	3.96	0.75	<0.03
HIP 32812	4977	4.41	0.56	-0.02	4.25	0.79	<-0.01
HIP 33392	4986	4.54	0.97	-0.09	4.01	0.77	<0.13
HIP 35992	4939	4.25	0.62	-0.02	4.55	0.79	<-0.01
HIP 5114	4846	4.39	0.74	-0.69	4.36	0.70	<-0.49
HIP 54446	4992	4.51	0.74	-0.18	4.36	0.76	<1.02
HIP 69224	5005	4.30	0.32	-0.14	4.55	0.78	<0.32
HIP 78242	5244	4.40	0.73	-0.01	4.50	0.86	<0.31
HD 109368	4651	4.36	0.67	-0.23	4.33	0.70	<-0.30
HD 116963	4735	4.43	0.51	-0.06	4.16	0.73	<-0.10
HD 117938	4738	4.27	0.36	-0.13	4.78	0.74	<-0.10
HD 119291	4611	4.22	0.59	-0.10	4.15	0.70	<-0.27
HD 11938	4703	4.25	0.76	0.01	4.41	0.75	<-0.07
HD 120491	4680	4.49	0.40	-0.34	4.22	0.70	<-0.11
HD 125271	4779	4.33	0.36	-0.22	4.36	0.71	<0.21
HD 126829	4726	4.51	0.82	-0.14	4.31	0.72	<-0.18
HD 132411	4673	4.32	0.31	-0.29	4.57	0.70	<-0.01
HD 137010	4797	4.41	0.48	-0.22	4.10	0.71	<0.00
HD 151692	4737	4.40	0.55	-0.07	4.23	0.73	<-0.08
HD 152533	4822	4.36	0.40	-0.04	4.38	0.76	<-0.21
HD 154387	4719	4.50	0.08	-0.25	4.27	0.70	<-0.03
HD 160836	4791	4.49	0.92	-0.16	3.75	0.71	<-0.09
HD 16280	4754	4.39	0.56	-0.19	4.24	0.71	<-0.39
HD 168863	4905	4.40	0.56	0.16	4.50	0.82	<0.11
HD 16905	4867	4.35	0.51	0.15	4.32	0.80	<0.04
HD 176535	4727	4.36	0.54	-0.15	4.02	0.71	<-0.13
HD 185283	4848	4.37	0.27	-0.06	4.71	0.77	<-0.09
HD 187760	4618	4.45	0.23	-0.32	4.36	0.70	<0.00
HD 191285	4634	4.41	0.38	-0.28	4.32	0.70	<0.09
HD 191902	4691	4.25	0.31	-0.18	4.95	0.72	<-0.09
HD 193406	4728	4.50	0.54	-0.34	4.17	0.70	<-0.02
HD 200083	4828	4.42	0.42	-0.09	4.35	0.75	<-0.09
HD 200349	4844	4.50	0.59	-0.26	4.20	0.71	<-0.22
HD 202389	4732	4.43	0.49	-0.25	4.43	0.71	<-0.30
HD 202819	4737	4.40	0.59	-0.26	4.41	0.70	<-0.08
HD 207699	4874	4.36	0.63	-0.12	4.48	0.76	<0.01
HD 210573	4918	4.48	0.68	-0.07	4.31	0.77	<-0.15
HD 211583	4761	4.39	0.26	0.05	4.02	0.75	<0.14
HD 214383	4876	4.47	0.59	-0.16	4.08	0.74	<0.28
HD 215722	4728	4.40	0.71	-0.10	3.95	0.71	<-0.13
HD 219495	4787	4.40	0.93	0.13	4.22	0.77	<0.16
HD 224432	4828	4.38	0.58	-0.06	4.39	0.76	<-0.20
HD 22897	4837	4.44	0.69	-0.25	4.22	0.71	<0.19
HD 23472	4813	4.38	0.43	-0.19	4.60	0.73	<-0.02
HD 297396	4717	4.30	0.46	0.06	4.26	0.75	<-0.12
HD 29985	4678	4.39	0.65	-0.22	4.01	0.70	<0.03
HD 30523	4662	4.57	0.79	-0.16	3.96	0.70	<0.09
HD 42505	4738	4.40	0.61	-0.22	4.09	0.70	<0.17
HD 45977	4689	4.30	0.52	0.03	4.47	0.75	<-0.14
HD 4838	4704	4.63	0.76	-0.21	4.22	0.70	<-0.04
HD 73583	4695	4.50	0.71	-0.21	4.53	0.71	<-0.08
BD -002387	4833	4.47	0.85	0.03	4.06	0.76	<0.02
BD -010184	4728	4.34	0.40	-0.34	4.55	0.70	<-0.14
BD -044138	4604	4.39	0.38	-0.11	3.92	0.70	<0.06
BD -053176	4758	4.39	0.82	-0.09	4.24	0.73	<0.04

Table 6. continued.

Star	T_{eff} (K)	$\log g$ (cm s^{-2})	ξ_t (km s^{-1})	[Fe/H]	Age (Gyr)	Mass (M_{\odot})	$A(\text{Li})$
BD -053596	4594	4.32	0.27	-0.34	4.36	0.70	<-0.19
BD -063481	4815	4.36	0.41	-0.14	4.62	0.74	<-0.50
BD -064196	4688	4.30	0.42	-0.03	4.68	0.75	<-0.18
BD -064756	4646	4.54	0.70	-0.23	4.18	0.70	<-0.25
BD -090872	4660	4.35	0.77	-0.19	4.18	0.70	<-0.23
BD -092670	4806	4.46	0.51	-0.08	4.17	0.74	<-0.12
BD -094191	4804	4.44	0.63	-0.32	4.52	0.71	<-0.08
BD -130116	4615	4.33	0.61	-0.49	4.20	0.70	<0.29
BD -140184	4714	4.32	0.76	-0.38	4.52	0.70	<0.04
BD -145003	4640	4.41	0.35	-0.51	4.32	0.70	<-0.14
BD -173242	4627	4.48	0.31	-0.29	4.32	0.70	<-0.09
BD -195953	4775	4.51	0.71	-0.14	4.44	0.73	<0.06
BD -213153	4622	4.38	0.76	-0.17	4.20	0.70	<0.31
BD -223528	4747	4.28	0.63	-0.17	4.26	0.71	<-0.19
HIP 102025	4684	4.32	0.53	-0.28	4.70	0.70	<-0.14
HIP 102964	4797	4.43	0.72	-0.23	4.43	0.72	<-0.16
HIP 103867	4559	4.14	0.77	-0.45	4.24	0.70	<-0.25
HIP 105506	4840	4.37	0.22	-0.01	4.27	0.76	<-0.18
HIP 109149	4960	4.43	0.32	-0.12	3.75	0.75	<0.16
HIP 109421	4576	4.42	0.32	-0.27	4.31	0.70	<-0.35
HIP 113596	4580	4.25	0.67	-0.21	4.27	0.70	<-0.26
HIP 116374	4626	4.31	0.42	0.01	3.99	0.70	<-0.12
HIP 17346	4699	4.32	0.66	-0.16	4.16	0.70	<-0.08
HIP 18918	4572	4.28	0.45	-0.20	4.40	0.70	<-0.11
HIP 25612	4571	4.35	0.56	-0.50	4.28	0.70	<-0.10
HIP 26013	4891	4.41	0.90	0.02	4.34	0.79	<-0.14
HIP 36347	4719	4.38	0.84	-0.05	3.84	0.72	<-0.06
HIP 38324	4615	4.39	0.48	-0.30	4.30	0.70	<-0.18
HIP 39470	4571	4.40	0.61	-0.39	4.17	0.70	<-0.23
HIP 45301	4788	4.46	0.10	-0.12	4.45	0.74	<0.06
HIP 54597	4799	4.43	0.52	-0.22	4.28	0.71	<0.73
HIP 57688	4712	4.32	0.37	-0.14	4.17	0.71	<-0.72
HIP 58348	4828	4.34	0.43	0.00	4.20	0.76	<-0.18
HIP 59925	4590	4.40	0.43	-0.26	4.30	0.70	<-0.14
HIP 61406	4855	4.42	0.68	0.03	4.19	0.77	<0.02
HIP 67126	4681	4.20	0.27	-0.19	5.02	0.72	<-0.24
HIP 7058	4749	4.55	0.41	-0.10	3.79	0.71	<-0.07
HIP 7743	4692	4.39	0.74	-0.17	4.60	0.71	<-0.16
HIP 96240	4849	4.47	0.70	-0.15	4.32	0.74	<-0.38
HD 283	5157	4.51	0.45	-0.54	5.30	0.72	<0.07
HD 750	5060	4.39	0.59	-0.29	5.20	0.75	<0.39
HD 870	5381	4.42	0.79	-0.10	3.04	0.87	<0.13
HD 2025	4939	4.58	0.61	-0.35	4.29	0.72	<-0.23
HD 3569	5155	4.54	0.60	-0.32	4.91	0.76	<0.03
HD 6348	5107	4.51	0.07	-0.56	5.16	0.71	<-0.69
HD 6673	4960	4.49	0.58	-0.26	4.48	0.74	<-0.21
HD 8326	4971	4.48	0.81	0.02	4.41	0.80	<0.09
HD 8389A	5283	4.37	1.06	0.34	5.37	0.91	<0.73
HD 8828	5403	4.46	0.72	-0.16	4.95	0.85	<0.20
HD 8859	5502	4.41	0.77	-0.09	4.89	0.89	<0.66
HD 8912	5211	4.43	0.70	-0.07	3.64	0.83	<0.18
HD 9246	4999	4.49	0.13	-0.53	4.27	0.70	<0.30
HD 9796	5179	4.38	0.66	-0.25	4.91	0.78	<0.17
HD 10002	5313	4.40	0.82	0.17	4.69	0.91	<0.49
HD 10166	5221	4.48	0.74	-0.39	3.37	0.76	<0.29
HD 11683	5007	4.42	0.60	-0.21	4.75	0.76	1.37
HD 12345	5395	4.44	0.69	-0.21	4.46	0.84	<0.05
HD 12617	4890	4.46	0.75	0.10	4.29	0.79	<0.02
HD 13060	5255	4.34	0.82	0.02	3.75	0.86	<-0.31
HD 13789	4740	4.33	0.79	-0.06	4.60	0.75	<-0.30
HD 14374	5425	4.48	0.81	-0.04	4.00	0.89	<0.75
HD 14635	4806	4.45	0.78	-0.03	3.95	0.74	<0.10
HD 14680	5011	4.46	0.69	-0.17	4.32	0.77	<0.35
HD 14744	4923	4.45	0.44	-0.13	5.01	0.77	<-0.06
HD 15337	5179	4.39	0.70	0.06	3.89	0.85	<0.42

Table 6. continued.

Star	T_{eff} (K)	$\log g$ (cm s $^{-2}$)	ξ_t (km s $^{-1}$)	[Fe/H]	Age (Gyr)	Mass (M_{\odot})	$A(\text{Li})$
HD 16270	4786	4.39	0.84	0.06	4.38	0.77	<0.03
HD 16297	5422	4.47	0.80	-0.01	5.33	0.89	<0.21
HD 16714	5518	4.42	0.76	-0.20	7.52	0.85	<0.23
HD 18386	5457	4.39	0.92	0.14	2.13	0.95	<0.42
HD 18719	5241	4.41	0.92	-0.08	5.07	0.83	<0.21
HD 21019	5468	3.93	1.05	-0.45	6.58	1.07	1.39
HD 21209A	4671	4.31	0.54	-0.41	4.46	0.70	<-0.56
HD 21411	5473	4.51	0.81	-0.26	8.36	0.82	<0.78
HD 21749	4723	4.40	0.53	-0.02	4.32	0.73	<-0.09
HD 22610	5043	4.44	0.88	-0.22	4.14	0.76	<-0.21
HD 23356	5004	4.50	0.87	-0.17	4.12	0.77	<-0.09
HD 24331	4965	4.51	0.53	-0.31	4.78	0.73	<-0.04
HD 25105	5316	4.47	0.77	-0.15	4.57	0.83	<-0.04
HD 25120	5134	4.47	0.87	-0.18	4.84	0.79	<0.61
HD 25565	5212	4.47	0.80	0.03	3.63	0.85	<0.38
HD 25673	5136	4.47	0.56	-0.50	4.20	0.73	<0.04
HD 30278	5394	4.39	0.72	-0.17	10.37	0.83	<0.23
HD 30306	5529	4.32	0.89	0.17	9.78	0.94	<0.52
HD 31560	4751	4.33	0.64	-0.07	4.71	0.73	<-0.13
HD 33725	5274	4.41	0.71	-0.17	6.91	0.82	<0.16
HD 34688	5169	4.44	0.70	-0.20	4.35	0.79	<0.22
HD 35854	4928	4.46	0.54	-0.13	4.95	0.77	<-0.22
HD 37986	5507	4.29	0.92	0.26	3.61	0.97	<0.65
HD 44573	5071	4.48	0.80	-0.07	4.06	0.80	<-0.01
HD 48611	5337	4.51	0.69	-0.36	4.47	0.79	<0.24
HD 52919	4698	4.37	0.67	-0.17	4.33	0.71	<-0.28
HD 65277	4802	4.43	0.55	-0.31	4.48	0.71	<-0.14
HD 68607	5215	4.41	0.82	0.07	4.31	0.86	<0.03
HD 71835	5438	4.39	0.79	-0.04	5.91	0.88	<0.63
HD 72579	5449	4.27	0.84	0.20	9.46	0.92	<0.61
HD 72673	5243	4.46	0.60	-0.41	10.26	0.75	<-0.17
HD 74014	5561	4.33	0.90	0.22	5.23	0.98	<0.32
HD 80883	5233	4.44	0.80	-0.25	6.31	0.80	<0.28
HD 81639	5522	4.40	0.79	-0.17	7.26	0.86	<0.60
HD 82516	5104	4.46	0.71	0.01	5.05	0.83	<0.02
HD 85119	5425	4.52	0.93	-0.20	3.12	0.85	1.38
HD 86065	5026	4.50	0.91	-0.06	3.72	0.79	<0.07
HD 86140	4903	4.55	0.31	-0.25	4.19	0.73	<-0.22
HD 86171	5400	4.47	0.81	-0.25	4.28	0.83	<0.98
HD 87521	4854	4.37	0.76	-0.04	4.28	0.76	<0.07
HD 88656	5150	4.44	0.81	-0.11	5.53	0.81	<0.24
HD 90711	5444	4.40	0.92	0.24	2.74	0.95	<0.58
HD 90812	5164	4.48	0.64	-0.36	4.28	0.75	<-0.06
HD 94151	5583	4.38	0.83	0.04	8.38	0.92	<0.42
HD 97343	5410	4.39	0.82	-0.06	10.39	0.85	<0.12
HD 98281	5381	4.42	0.64	-0.26	8.85	0.81	<0.04
HD 98356	5322	4.41	0.84	0.10	4.19	0.89	<0.53
HD 100508	5449	4.42	0.86	0.39	5.36	0.95	<0.59
HD 101581	4738	4.46	0.66	-0.52	4.13	0.70	<-0.29
HD 102438	5560	4.41	0.84	-0.29	11.40	0.82	<-0.08
HD 103949	4881	4.48	0.49	-0.07	4.20	0.76	<-0.17
HD 105671	4748	4.42	0.90	-0.02	4.13	0.73	<-0.08
HD 106275	5059	4.47	0.67	-0.09	5.18	0.80	<-0.03
HD 109200	5134	4.51	0.68	-0.31	6.92	0.76	<-0.14
HD 109423	5074	4.44	0.87	-0.07	3.53	0.80	<-0.31
HD 112540	5523	4.52	0.74	-0.17	5.75	0.87	<0.28
HD 116858	4990	4.52	0.77	-0.21	4.63	0.76	<-0.24
HD 116920	5015	4.46	0.68	-0.23	4.36	0.76	<-0.17
HD 119782	5160	4.44	0.79	-0.07	6.01	0.82	<-0.42
HD 124106	5106	4.49	0.80	-0.17	5.06	0.79	<-0.88
HD 124292	5443	4.37	0.77	-0.13	10.39	0.85	<-0.50
HD 124364	5584	4.48	0.83	-0.27	4.05	0.86	1.23
HD 125072	5007	4.56	1.04	0.18	4.25	0.82	<0.36
HD 125455	5162	4.52	0.70	-0.18	5.62	0.80	<-0.64
HD 128674	5551	4.50	0.71	-0.38	10.90	0.80	<0.86

Table 6. continued.

Star	T_{eff} (K)	$\log g$ (cm s^{-2})	ξ_t (km s^{-1})	[Fe/H]	Age (Gyr)	Mass (M_{\odot})	$A(\text{Li})$
HD 130992	4898	4.54	0.71	-0.13	4.04	0.75	<-0.20
HD 132648	5418	4.49	0.69	-0.37	9.55	0.78	<0.52
HD 136713	4994	4.45	0.94	0.07	4.33	0.81	<0.10
HD 136894	5412	4.36	0.75	-0.10	9.74	0.85	<-0.36
HD 137303	4756	4.51	0.40	-0.35	4.62	0.70	<-0.41
HD 142709	4728	4.44	0.84	-0.35	4.35	0.70	<-0.22
HD 143295	4987	4.43	0.89	-0.03	3.99	0.79	1.24
HD 144411	4852	4.39	0.05	-0.32	4.28	0.71	<-0.28
HD 144497	5022	4.50	0.82	-0.12	4.48	0.78	-0.28
HD 144628	5085	4.51	0.55	-0.41	5.16	0.74	<-0.29
HD 147512	5530	4.40	0.81	-0.08	9.93	0.87	<0.40
HD 148303	4958	4.55	0.84	-0.03	4.41	0.79	<0.86
HD 151504	5457	4.36	0.87	0.06	8.73	0.90	<0.47
HD 153851	5052	4.50	0.91	-0.25	4.80	0.76	<0.06
HD 154577	4900	4.52	0.42	-0.70	6.02	0.70	<-0.51
HD 157830	5540	4.49	0.76	-0.25	5.12	0.85	<0.08
HD 161098	5560	4.46	0.79	-0.27	8.16	0.84	<0.47
HD 162236	5343	4.43	0.82	-0.12	4.20	0.85	<0.09
HD 165920	5339	4.39	0.79	0.29	5.14	0.92	<0.43
HD 167359	5348	4.46	0.67	-0.19	4.51	0.83	<0.05
HD 168159	4783	4.42	0.99	-0.15	4.05	0.72	0.91
HD 170493	4751	4.24	0.59	0.14	4.40	0.78	<-0.04
HD 172513	5500	4.41	0.79	-0.05	4.36	0.90	<0.46
HD 176157	5181	4.41	0.92	-0.16	5.00	0.81	<0.19
HD 176986	5018	4.45	0.82	0.00	4.47	0.81	<0.13
HD 183783	4595	4.29	0.05	-0.20	4.93	0.71	<-0.39
HD 183870	5029	4.49	0.78	-0.07	4.92	0.79	<-0.23
HD 186061	5016	4.51	0.62	-0.02	4.07	0.80	<0.19
HD 188559	4786	4.33	0.65	-0.11	4.39	0.74	<-0.27
HD 189242	4913	4.46	0.56	-0.38	5.14	0.72	<-0.26
HD 191847	5066	4.45	0.48	-0.12	4.17	0.79	<-0.14
HD 192117	5479	4.48	0.75	-0.04	3.54	0.90	<0.78
HD 192961	4624	4.31	0.58	-0.35	4.32	0.70	<-0.11
HD 193844	5007	4.44	0.48	-0.30	4.47	0.74	<-0.18
HD 195302	5063	4.44	0.64	0.02	4.32	0.82	<-0.12
HD 196761	5415	4.43	0.76	-0.31	11.29	0.79	<0.13
HD 197210	5577	4.42	0.86	-0.03	3.70	0.93	<0.51
HD 197823	5396	4.41	0.82	0.12	6.64	0.91	<0.29
HD 199933	4730	4.32	0.64	-0.15	4.37	0.72	<-0.09
HD 200505	5052	4.47	0.73	-0.45	4.62	0.72	<0.18
HD 203384	5586	4.40	0.90	0.26	2.77	1.00	<0.57
HD 203413	4812	4.39	0.74	0.01	4.38	0.76	<-0.13
HD 203850	4879	4.51	0.36	-0.68	4.93	0.70	<-0.60
HD 205536	5442	4.38	0.77	-0.05	9.37	0.87	<0.10
HD 206163	5519	4.43	0.94	0.01	2.20	0.94	<0.58
HD 207583	5534	4.46	0.99	0.01	2.99	0.93	<1.35
HD 208272	5199	4.42	0.99	-0.08	5.31	0.83	<-0.23
HD 208573	4910	4.41	0.86	0.00	4.31	0.78	<-0.16
HD 209100	4754	4.45	0.68	-0.20	4.18	0.71	<-0.39
HD 209742	5137	4.49	0.79	-0.16	4.93	0.80	<-0.14
HD 211369	4984	4.44	0.67	0.04	4.15	0.80	<0.12
HD 212563	5018	4.52	0.89	-0.02	4.07	0.80	1.56
HD 212580	5155	4.44	0.85	-0.11	4.05	0.81	<-0.01
HD 213628	5555	4.44	0.82	0.01	3.07	0.94	<0.73
HD 214759	5461	4.37	0.85	0.18	3.51	0.95	<0.54
HD 218249	5009	4.52	0.46	-0.40	4.31	0.72	<0.09
HD 218511	4556	4.31	0.41	-0.10	4.40	0.70	<-0.14
HD 218572	4785	4.54	0.50	-0.56	4.32	0.70	<0.16
HD 219249	5482	4.50	0.74	-0.40	8.16	0.79	<0.55
HD 220339	5029	4.55	0.76	-0.35	4.93	0.74	<-0.31
HD 222335	5271	4.49	0.83	-0.20	5.86	0.81	<0.16
HD 222422	5475	4.46	0.73	-0.12	3.58	0.88	<0.91
HD 223121	5077	4.34	0.74	0.05	4.15	0.82	<0.49
HD 223282	5328	4.49	0.60	-0.41	5.93	0.77	<0.48
HD 224619	5436	4.39	0.79	-0.20	9.49	0.83	<0.19

Table 6. continued.

Star	T_{eff} (K)	$\log g$ (cm s^{-2})	ξ_t (km s^{-1})	[Fe/H]	Age (Gyr)	Mass (M_{\odot})	$A(\text{Li})$
HD 224789	5185	4.44	1.05	-0.03	4.86	0.83	<0.06
HD 171587	5412	4.59	0.76	-0.64	7.40	0.77	1.26
HD 207869	5527	4.50	0.73	-0.45	4.28	0.81	<0.44
HD 113101	5456	4.37	0.66	-0.07	4.92	0.89	<0.54
HD 11397	5565	4.50	0.77	-0.55	5.56	0.80	<-0.07
HD 126681	5561	4.71	0.71	-1.14	4.68	0.71	1.52
HD 126803	5477	4.50	0.50	-0.61	6.31	0.78	<-0.28
HD 137676	5253	3.93	0.74	-0.53	11.19	0.93	<-1.16
HD 139189	5075	4.41	0.78	0.02	4.60	0.83	<-0.92
HD 139332	4899	4.30	0.04	0.00	4.34	0.79	<-0.53
HD 139536	5209	4.71	1.13	-0.04	4.27	0.84	<-0.46
HD 14452	5313	4.50	0.85	-0.16	4.53	0.84	<0.34
HD 163436	5030	4.43	0.45	-0.07	4.42	0.80	<-0.42
HD 197921	4913	4.36	0.34	0.13	4.57	0.82	<-0.24
HD 210320	5597	4.31	0.87	0.11	6.59	0.96	<0.56
HD 218750	5166	4.39	0.57	0.08	4.80	0.86	<-0.26
HD 223272	5118	4.41	0.58	0.13	4.35	0.85	<-0.08
HD 224063	5591	4.27	0.84	0.14	7.51	0.97	<0.19
HD 23901	5264	3.93	0.84	-0.40	11.17	0.93	<1.10
HD 24633	5276	4.36	0.59	-0.04	5.90	0.87	<-0.20
HD 291763	4987	4.50	0.12	-0.61	4.44	0.70	<-0.35
HD 324492	4962	4.15	0.52	-0.27	4.19	0.73	<-0.87
HD 329788	5151	4.35	0.19	-0.08	4.00	0.81	<0.11
HD 56380	5317	4.35	0.53	-0.42	6.28	0.79	<0.03
HD 61051	5363	4.37	0.70	-0.10	4.57	0.86	<-0.11
HD 63685	5497	4.05	0.94	0.00	9.78	1.01	<0.66
HD 75530	5311	4.48	0.53	-0.54	6.34	0.77	<-0.33
HD 82783	5318	4.41	0.91	0.21	3.92	0.91	<0.43
BD -082534	5405	4.43	0.41	-0.78	5.16	0.73	<0.69
HIP 104856	5023	4.43	0.22	-0.24	4.64	0.76	<0.18
HIP 31639	5400	4.53	0.31	-0.54	4.56	0.77	<0.61
HIP 32127	5302	4.44	0.58	-0.64	5.65	0.75	<0.11
HIP 41659	5197	4.38	0.42	-0.53	5.31	0.75	<0.15
HIP 88316	5159	4.38	0.35	-0.01	4.82	0.84	<0.35
HD 101650	4626	4.29	0.11	-0.45	4.09	0.70	<-0.26
HD 108935	4724	4.30	0.55	0.02	4.21	0.74	<-0.14
HD 147147	4856	4.51	0.71	-0.17	4.25	0.74	<0.71
HD 189987	4746	4.25	0.09	-0.06	4.92	0.75	<-0.04
HD 20492	4770	4.30	0.59	0.02	4.38	0.76	<-0.10
HD 214998	4847	4.37	0.77	0.06	4.24	0.78	<0.09
HD 326267	4719	4.31	0.45	-0.26	4.26	0.70	<-0.05
HD 57568	4821	4.51	0.38	-0.47	4.14	0.70	<-0.12
HD 58489	4800	4.33	0.59	0.10	4.32	0.77	<-0.01
HD 89668	4811	4.45	0.63	-0.11	4.02	0.73	<-0.08
HD 96673	4788	4.38	0.55	-0.13	4.40	0.73	<0.03
BD -012505	4741	4.51	0.44	-0.11	3.59	0.70	<0.21
BD -034797	4622	4.21	0.30	0.06	4.42	0.73	<-0.02
BD -050484	4674	4.42	0.21	-0.39	4.36	0.70	<-0.09
BD -120327	4680	4.35	0.57	-0.34	4.47	0.70	<0.02
BD -123458	4803	4.86	0.43	-0.83	3.25	0.70	<-0.01
BD -130321	4772	4.41	0.78	0.02	3.67	0.73	<0.14
HIP 108216	4830	4.53	0.66	-0.51	4.22	0.70	<-0.34
HIP 21934	4674	4.19	0.62	0.03	3.81	0.71	<-0.04
HIP 64965	4888	4.78	0.00	-1.03	4.01	0.70	<0.07
HIP 80083	4800	4.78	0.31	-0.80	4.10	0.70	<0.14
HIP 9398	4734	4.49	0.62	-0.43	3.79	0.70	<0.04
HD 967	5564	4.51	0.79	-0.68	8.39	0.78	<0.42
HD 8638	5507	4.43	0.74	-0.38	7.91	0.80	<0.05
HD 14747	5516	4.43	0.72	-0.39	11.20	0.79	<0.32
HD 17970	5040	4.39	0.29	-0.45	9.12	0.74	<-0.29
HD 19034	5477	4.40	0.69	-0.48	9.27	0.77	<-0.06
HD 24892	5363	3.99	0.88	-0.32	11.09	0.95	1.39
HD 26965A	5153	4.39	0.36	-0.31	10.80	0.77	<-0.34
HD 36003	4647	4.31	0.42	-0.20	4.53	0.70	<-0.32
HD 40397	5527	4.39	0.83	-0.13	10.69	0.86	<0.52

Table 6. continued.

Star	T_{eff} (K)	$\log g$ (cm s^{-2})	ξ_t (km s^{-1})	[Fe/H]	Age (Gyr)	Mass (M_{\odot})	$A(\text{Li})$
HD 50590	4870	4.39	0.35	-0.22	4.85	0.74	<-0.21
HD 65562	5076	4.39	0.45	-0.10	5.11	0.80	<-0.17
HD 82342	4820	4.41	0.30	-0.54	4.41	0.70	<-0.45
HD 104006	5023	4.56	0.15	-0.78	5.68	0.70	<-0.48
HD 104263	5477	4.34	0.81	0.02	9.11	0.89	<0.08
HD 114747	5172	4.44	0.98	0.21	3.74	0.87	<0.32
HD 123265	5338	4.29	0.85	0.19	4.78	0.91	<0.37
HD 129642	5026	4.49	0.69	-0.06	4.89	0.81	<-0.13
HD 130930	5027	4.45	0.50	0.01	4.94	0.82	<0.01
HD 134985	5090	4.44	0.10	-0.60	4.61	0.72	<-0.40
HD 145598	5417	4.48	0.59	-0.78	6.19	0.72	<-0.20
HD 174545	5216	4.40	0.88	0.22	6.34	0.89	<0.35
HD 185615	5570	4.34	0.84	0.08	6.28	0.94	<0.33
HD 187456	4832	4.33	0.56	0.02	4.50	0.78	<-0.15
HD 190954	5430	4.46	0.63	-0.41	7.75	0.78	<0.19
HD 192031	5215	4.39	0.04	-0.84	6.55	0.70	<0.02
HD 207970	5556	4.38	0.80	0.07	7.93	0.93	<0.39
HD 210975	4749	4.37	0.05	-0.43	4.31	0.70	<-0.54
HD 213042	4831	4.38	0.82	0.08	4.41	0.77	<0.06
HD 213941	5532	4.41	0.72	-0.46	11.38	0.79	<0.38
HD 219077	5362	4.00	0.92	-0.13	9.04	1.04	1.49
HD 220256	5144	4.41	0.47	-0.10	6.48	0.82	<-0.09
HD 222237	4780	4.37	0.05	-0.38	4.82	0.70	<-0.40
HD 967	5568	4.53	0.77	-0.68	8.39	0.78	<-0.18
HD 68089	5597	4.53	0.66	-0.77	6.25	0.77	<1.01
HD 108564	4818	4.67	0.26	-0.97	4.35	0.70	<-0.20
HD 111515	5398	4.47	0.71	-0.61	7.59	0.77	<0.25
HD 131653	5324	4.54	0.35	-0.66	4.48	0.73	<0.09
HD 175607	5392	4.51	0.60	-0.62	8.14	0.77	<-0.14
CD -452997	5312	4.39	0.24	-0.84	—	—	<0.45